ORIGINAL PAPER

Determination of future creep and seismic behaviors of dams using 3D analyses validated by long-term levelling measurements

Murat Cavuslu[1] · **Samed Inyurt**[2]

Abstract

This study aims to assess the future structural performance of the Kozlu-Ulutan clay core rockfill (CCR) dam, one of the most significant water structures in the Black Sea region of Turkey, by utilizing 35 years of levelling measurements and 3D finite-difference analyses. Settlement measurements were obtained from five different points on the dam surface every 6 months. Subsequently, a three-dimensional (3D) model of the dam was created using the finite-difference method. Time-dependent creep analyses and seismic analyses were conducted sequentially, employing the Burger-Creep and Mohr–Coulomb material models, respectively. Non-reflecting boundary conditions were defined for the boundaries of the dam model. The 3D numerical analysis results were found to be highly compatible with the 35 years of levelling measurements. Additionally, the future seepage and settlement behaviors of the dam over a 100-year period (2023–2123) were analyzed, considering special time functions. Current and future seismic analyses were performed, taking into account the settlement results of the dam in 2023 and 2123. For seismic analyses, data from ten various earthquakes that occurred in Kahramanmaraş, Hatay, Malatya, and Gaziantep in Turkey in 2023 were utilized. The seismic analysis results provided significant information about the future seismic behavior of the Kozlu-Ulutan Dam, revealing notable differences between the current and future earthquake behaviors of the dam. Moreover, it was concluded that the clay core is the most crucial section concerning the current and future seismic behaviors of CCR dams. The study results emphasized the importance of continuous monitoring and periodic seismic evaluations for the safe operation of CCR dams.

Keywords Clay core rockfill dam · Finite-difference modeling · Levelling measurement · Non-reflecting boundary condition · Seismic analysis

1 Introduction

Dams play a critical role in supporting various ecosystems and human activities, establishing themselves as essential water infrastructure worldwide. Consequently, dam engineers have increasingly prioritized the static and dynamic safety of these structures, especially in recent decades. There exist diverse types of dams globally, including clay core rockfill dams and concrete dams, each possessing distinct advantages and disadvantages. Among these, clay core rockfill (CCR) dams stand out as widely utilized structures. Constructed by compacting various soil, rock, and other materials, CCR dams form embankments designed to withstand environmental forces, such as earthquakes and floods, while ensuring durability and stability. Notably, CCR dams offer cost-effectiveness compared to concrete dams and boast easier construction processes utilizing local materials and less specialized labor. Additionally, their environmental impact during both construction and operation remains relatively low. However, CCR dams face unique challenges and risks, particularly concerning stability. Factors such as settlement and liquefaction of soil and rock materials utilized in their construction can compromise their stability, potentially leading to modes of failure like overtopping, sliding, or collapse. Consequently, meticulous monitoring and ongoing assessment of the safety and stability of CCR dams are imperative over time.

✉ Murat Cavuslu
murat.cavusli@beun.edu.tr

✉ Samed Inyurt
samed.inyurt@gop.edu.tr

1   Department of Civil Engineering, Zonguldak Bulent Ecevit University, Zonguldak, Turkey

2   Department of Geomatics Engineering, Tokat Gaziosmanpaşa University, Tokat, Turkey

Monitoring the time-dependent creep, settlement, and seismic behaviors of dams is of paramount importance in ensuring their structural integrity and long-term stability. Creep, characterized by slow deformation under sustained load over time, can lead to gradual changes in dam geometry and internal stresses, potentially compromising its structural integrity. Settlement, another critical parameter, reflects the gradual compression and consolidation of the dam foundation and materials, which can affect its overall stability and performance. Additionally, seismic events pose a significant threat to dam safety, as ground shaking can induce dynamic forces and deformations that may exceed the design limits, resulting in catastrophic failure. Continuous monitoring of these behaviors allows for early detection of potential issues, enabling proactive maintenance and remedial measures to be implemented to mitigate risks and ensure the safety and reliability of dams. Furthermore, understanding the long-term trends and patterns in creep, settlement, and seismic responses provides valuable insights into the evolving behavior of dams under varying environmental and loading conditions, aiding in the refinement of design criteria and risk assessment protocols. In summary, the comprehensive monitoring of time-dependent creep, settlement, and seismic behaviors plays a crucial role in safeguarding the integrity and performance of dams, ultimately contributing to the protection of lives, property, and critical infrastructure.

In recent years, advancements in technology and modeling techniques have facilitated the analysis and prediction of the behavior of CCR dams under diverse loading conditions. These advancements include 3D finite difference settlement analysis, enabling the simulation of deformation and stress distribution within the dam over time. Additionally, levelling measurements can be employed to monitor vertical deformations and movements of the dam's surface. Despite these advancements, there remains a paucity of studies in the literature examining the current and future failure behaviors of CCR dams using levelling measurement results. Cetin et al. [1] investigated the settlement performance of a rockfill dam, observing a maximum settlement of approximately 2.7 m on the crest section of the dam body between 1992 and 1997. Mahinroosta et al. [2] proposed a methodology to estimate the settlement of rockfill dams during the initial filling stage, suggesting that initial impoundment should proceed gradually to ensure safer conditions. Liu et al. [3] examined the stress–strain behavior of rockfill dams through numerical stress-deformation analyses, noting friction between the cut-off wall and the surrounding foundation due to uneven settlement. Neves and Pinto [4] demonstrated the reliability of predicting collapse settlements in rockfill dams resulting from saturation of the rockfill embankments, concluding that such predictions are feasible and reliable. Habibagahi [5] analyzed the post-construction settlement behavior of four

different types of rockfill dams, indicating that adaptive network-based fuzzy inference systems are more reliable and accurate than conventional methods. Haeri and Faghihi [6] compared monitoring and numerical analyses of the Taleghan rockfill dam during construction, finding that unsaturated and double-surface plasticity soil models provide better predictions of core behavior than elastic and single-surface elastoplastic models. Dolezalova and Hladik [7] assessed the long-term safety of a 62-m-high rockfill dam through monitoring and simulation with calibrated 2D and 3D models. The modeling results were instrumental in analyzing slope stability, estimating the hazard of clay core cracking and hydraulic fracturing, and informing the rehabilitation concept and project of the dam. Rashidi and Haeri [8] delved into the nonlinear behavior of earth and rockfill dams during construction and initial impounding phases, utilizing instrumentation data and numerical modeling. Their findings revealed that 88% of the total settlement occurred during the construction period, with a maximum core settlement of 238 cm at the end of construction and a cumulative settlement of 270 cm over 6 years of exploitation. In a separate investigation, Wei et al. [9] examined the behavior of high-earth core dams using a generalized plasticity model under both static and dynamic loading conditions. The study demonstrated the model's ability to accurately simulate stress paths of dam materials, including acceleration response and residual deformation during design earthquakes, consistent with engineering experience. Pinyol and Alonso [10] focused on the design, construction, monitoring, and modeling of an earth dam, achieving good agreement between calculations and measurements by identifying the compressibility of different compacted materials and the foundation rock. However, larger settlements were observed downstream than expected when the dam reached an elevation of 350 m. Liu et al. [11] conducted laboratory tests to simulate the behavior of rockfill dams under various loading conditions, considering the breakage of rock particles. They developed a numerical model using the finite element method, demonstrating that particle breakage significantly affects the dam's deformation and stability, with the numerical model accurately predicting the dam's behavior. Feng et al. [12] employed a three-dimensional conditional random field to model the spatial variability of soil properties and conducted a random finite element analysis to evaluate the rockfill dam's safety performance. The results indicated that the safety factor of the clay-core-wall rockfill dam decreases with increasing spatial variability of soil properties. Li et al. [13] gathered spatial–temporal data from multiple monitoring points within a rockfill dam and developed multiple-monitoring-point models to analyze settlement behavior. These models incorporated the spatial and temporal variability of settlement data, with

results demonstrating the accurate prediction of failure point settlement in rockfill dams. Chen et al. [14] devised a novel method for monitoring internal deformation in earth-rockfill dams using high-precision flexible pipeline measurements. Through laboratory tests and numerical simulations, they evaluated the method's performance, revealing that flexible pipeline sensors accurately measure internal deformation and offer valuable insights into dam deformation behavior. In a separate study, Chen et al. [15] conducted numerical analyses on the deformation and stability of a rockfill dam with leakage issues. Utilizing a three-dimensional finite element model, they simulated the dam's behavior under various leakage scenarios, finding that leakage significantly influences deformation and stability, with increased flow rates leading to decreased safety factors. Costigliola et al. [16] introduced a new approach to predicting long-term settlements of dams by combining laboratory and field tests. Employing empirical and numerical methods, they evaluated the effectiveness of this approach, demonstrating its utility in predicting permanent settlements of upstream-faced earth dams, thereby serving as a valuable tool for design and construction. Guan et al. [17] investigated the deformation and damage behavior of deep concrete cut-off walls in the foundations of core earth-rock dams. Using a plastic damage model, they simulated the behavior of concrete cut-off walls under various loading conditions. Through field monitoring data and numerical simulations, they analyzed the deformation and damage behavior of concrete cut-off walls in a large-scale core earth-rock dam case study. The results of the study underscored the significant influence of the plastic damage model on the deformation and damage behavior of concrete cut-off walls. Xu et al. [18] conducted a full-scale settlement test, utilizing the results for back-analysis to determine foundation and embankment material parameters. They identified initial settlement, soil type, and stress level as primary factors influencing long-term foundation settlement, with the settlement behavior influenced by the deformation characteristics of the rockfill embankment. Yao et al. [19] investigated the long-term deformation behavior of the Shuibuya rockfill dam in China. Employing the response surface method and an improved genetic algorithm, they identified critical factors affecting dam deformation. Through a developed 3D finite element model and comparison with monitoring system data, their research demonstrated the effectiveness of predicting long-term deformation behaviors of rockfill dams, highlighting dam height, rockfill elastic modulus, and Poisson's ratio as significant influencing factors. Sukkarak et al. [20] proposed a modified valley shape factor (VSF) for more accurate settlement estimation in rock-fill dams, considering the shape of the dam valley's impact on settlement behavior. Validated using data from three case studies, the modified VSF method exhibited superior results compared to conventional methods, offering a useful tool for designers and engineers to estimate rockfill dam settlement more accurately.

While the literature review highlights advancements in settlement estimation methods, minimal research has focused on verifying current and future settlement behavior of rockfill dams through long-term levelling measurements, as well as predicting their future seismic behavior. Therefore, this study aims to address these deficiencies in the literature and provide detailed insights to researchers regarding future settlement and seismic behavior of CCR dams.

2 General information about Kozlu-Ulutan Dam

The Zonguldak Kozlu-Ulutan Dam is a clay-core rockfill dam situated on the eastern coast of the Black Sea in Turkey. (Fig. 1) Constructed in 1986 by DSI (State Hydraulic Works) for hydroelectric power generation, flood control, and irrigation purposes, the dam project encompasses a total filling material volume of 24 million m^3, along with three diversion tunnels measuring 12 m in diameter and 1 km in length, and three power tunnels with an 11 m diameter [22]. Positioned within a precipitation area of 35,509 km^2, the dam is located approximately 25 km east of Zonguldak city and 3 km south of Kozlu. With a crest width of 8 m and a height reaching 130 m, its reservoir boasts a volume of around 10.4 billion m^3, a maximum water elevation of 526.82 m, and a reservoir area spanning 318.5 km^2. The project has an installed capacity of 1200 MW, expected to generate an average of 3.833 GWh of power annually. The dam's body exhibits varying depths along the crest, with upstream and downstream slopes set at 1:1.4, and slopes of 2:1.5 for the rockfill and transition zones. Founded on rock formations predominantly comprising sandstones and conglomerates, the dam's foundation is structured with a rockfill zone overlaid by a filter and drainage layer, while its core comprises clayey silt and sand material. Figure 2 provides a detailed depiction of the typical cross-section and height of the dam body [22], while Fig. 3 illustrates the water levels of the Kozlu-Ulutan Dam. Safety-wise, the dam adheres to modern dam safety standards in design and construction, overseen and maintained by the General Directorate of State Hydraulic Works of Turkey [22], with regular inspections and maintenance conducted to ensure continued safe operation. Overall, the Kozlu-Ulutan Dam stands as a crucial infrastructure project delivering substantial benefits to the region in electricity generation, flood control, irrigation, and recreation. Detailed material properties of the dam are presented in Table 1.
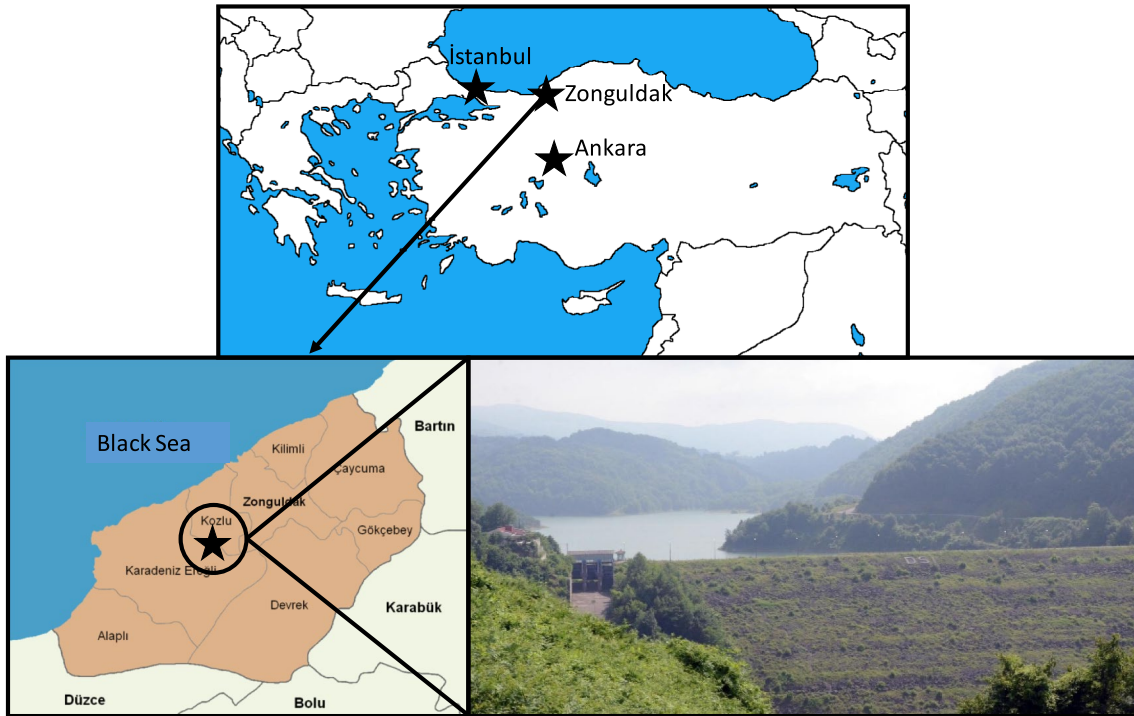
Fig. 1 The general view of the Kozlu-Ulutan Dam [22, 27]

Fig. 2 The most critical section of the Kozlu-Ulutan Dam [22]
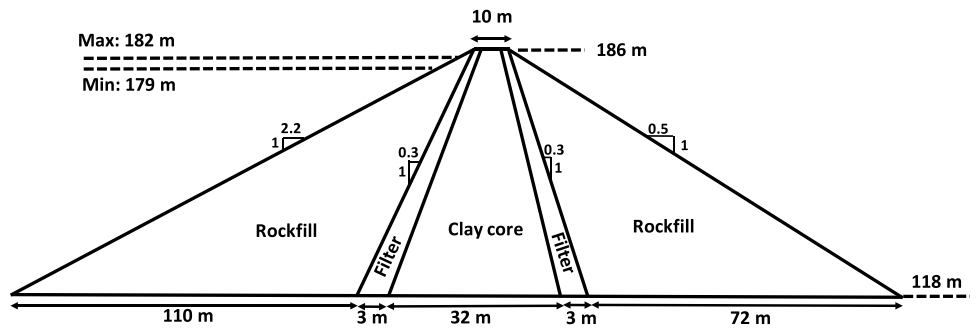
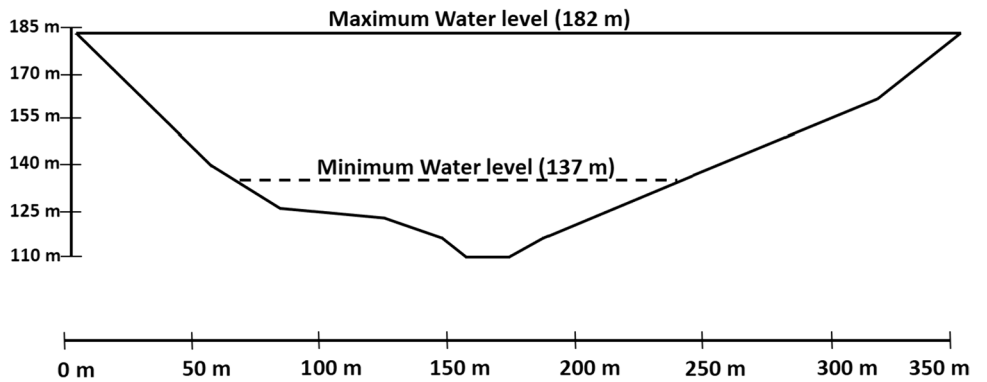

Fig. 3 Changes in water levels in the Kozlu-Ulutan dam [22]

Table 1 Material properties of the Kozlu-Ulutan dam body [8, 22, 26, 27]

Characteristics	$\Delta\Phi$ (°)	c (kPa)	ρ (t/m³)	ρ_{sat} (t/m³)	E_s (MPa)	υ	Dilation angle (°)
Clay core	26	52	1.62	1.74	24	0.32	0
Filter material	36	0	2.03	2.17	115.2	0.27	3
Upstream rockfill	42	0	2.12	2.25	187.5	0.23	8
Downstream rockfill	42	0	2.12	2.25	187.5	0.23	8
Foundation	45	0	2.26	2.38	2130	0.21	9

$\Delta\Phi$ Internal friction angle, c Cohesion, ρ Natural density, ρ_{sat} Saturation density, E_s Deformation modulus, υ Poisson ratio

3 Seismicity of the zone

Turkey is situated within the Mediterranean–Alpine–Himalayan Belt, an active seismic region characterized by complex tectonic activity, which results in frequent earthquakes. Throughout history, Turkey has experienced numerous significant earthquakes, leading to extensive damage and loss of life. The seismicity in Turkey is primarily attributed to the interaction of several tectonic plates, including the African, Arabian, Eurasian, and Anatolian plates, converging and interacting to create high tectonic activity, particularly along the North Anatolian Fault Zone (NAFZ) and East Anatolian Fault Zone (EAFZ). The Kozlu-Ulutan Dam is situated within the NAFZ, highlighting the importance of assessing its seismic behavior for future safety and security (Fig. 4). According to Fig. 4, the NAFZ is one of the most significant geological features in Turkey, playing a crucial role in shaping the country's seismic landscape. Extending approximately 1500 km along the northern coast of Turkey, the NAFZ is a major right-lateral strike-slip fault system that extends from the Aegean Sea in the west to the east of the Black Sea. This fault zone represents a complex geological structure where the Anatolian Plate interacts with the Eurasian Plate. The NAFZ is characterized by its segmented nature, divided into several distinct segments, each exhibiting unique seismic behavior and potential for earthquake activity. These segments include the Eastern Marmara segment, Central Anatolian segment, and Eastern Anatolian segment, among others. Each segment may produce earthquakes independently, adding to the complexity of seismic hazard assessment in the region. The NAFZ accommodates the relative motion between the Anatolian Plate and the Eurasian Plate, with the Anatolian Plate moving westward relative to the Eurasian Plate. This horizontal motion results in frequent earthquakes along the fault segments, with significant strain accumulation over time leading to periodic seismic events. Historically, the NAFZ has been responsible for several devastating earthquakes in Turkey, including the 1999 İzmit earthquake and the 1999 Düzce earthquake, which resulted in significant loss of life and widespread destruction. These events underscore the importance of understanding the seismic hazard posed by the NAFZ and implementing effective mitigation strategies to minimize the impact of future earthquakes on vulnerable communities and infrastructure. Overall, the NAFZ stands as a critical geological feature

Fig. 4 Seismic fault map of Türkiye [23]
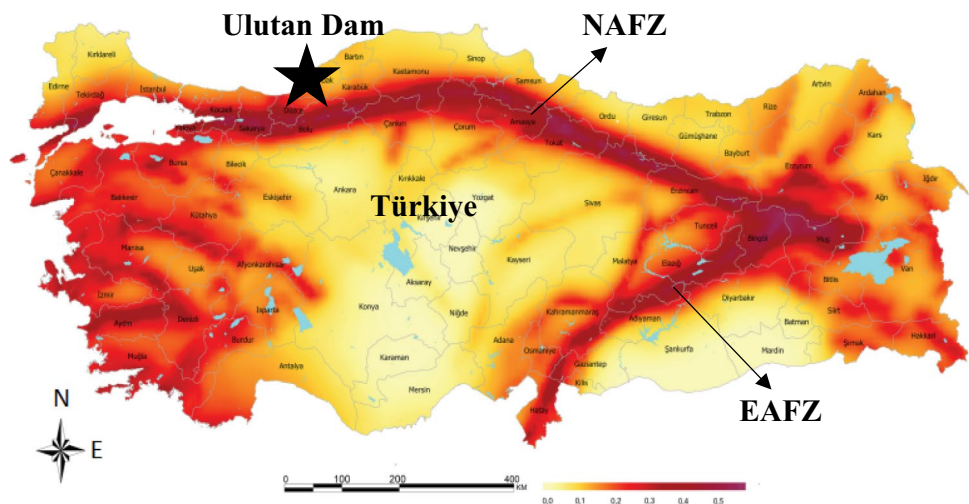
in Turkey, highlighting the country's susceptibility to seismic activity and the importance of ongoing research and monitoring efforts to mitigate earthquake risk and ensure the safety and resilience of affected regions.

4 General information about levelling measurements and time-dependent settlement results

The occurrence of time-dependent vertical displacements on a dam, resulting from factors such as changes in water levels, soil erosion, or temperature changes, can significantly affect its safety and stability. Monitoring these displacements over time is crucial to ensure the dam's stability and safety, as failure to do so can lead to structural damage, environmental and economic consequences, and loss of life. Engineers and surveyors can identify areas at risk of failure by tracking these displacements and take appropriate measures, including reinforcing the dam, repairing damage, or adjusting water levels in the reservoir to alleviate stress on the structure. The Kozlu-Ulutan Dam, a critical water structure serving the western Black Sea region, underscores the importance of continuous monitoring of its behavior. Levelling observations should be considered in predicting the future behaviors of clay core rockfill (CCR) dams like Kozlu-Ulutan to understand the current situation of the dam. This study provides comprehensive information on the deformation measurements of the Kozlu-Ulutan Dam over 35 years, employing the levelling method. Construction

of the Kozlu-Ulutan Dam was completed in 1988, and vertical displacements on the dam body have been periodically observed and monitored since then. The General Directorate of State Hydraulic Works [22] recorded vertical displacements on the dam body between 1988 and 2023 to track settlement changes over time. Settlement monitoring occurred in June and December of each year for 35 years, focusing on five different nodal points on the dam body surface strategically selected based on their location and deformation sensitivity, as illustrated in Fig. 5.

To ensure the accurate monitoring of settlements on clay core rockfill dams, it is imperative to select appropriate measurement points. Five points, positioned 5 m below the crest where the maximum water level occurs, were chosen for this purpose. In 1988, these geodetic points were fixed using concrete molds. The levelling data, graphically represented in Fig. 6, offer a comprehensive visualization of settlement changes over the monitoring period. This data facilitates a deeper understanding of the Kozlu-Ulutan Dam's behavior over time and aids in assessing the long-term stability of this critical water structure. Point 1, located on the right side of the dam, exhibited detailed settlement values in Fig. 6a. Following the dam's initial water retention between 1988 and 1989, the maximum settlement value on Point 1 was recorded at 2.31 cm. Settlements on Point 1 increased rapidly until 2003, after which the rate of increase decreased notably. By 2004, the largest settlement value on Point 1 reached 30 cm, and by 2023, it peaked at 36.4 cm, with no significant changes observed after 2020. Figure 6b illustrates time-dependent settlement changes on Point 2

Fig. 5 Kozlu-Ulutan Dam's top view and view of 5 various points on the dam body surface
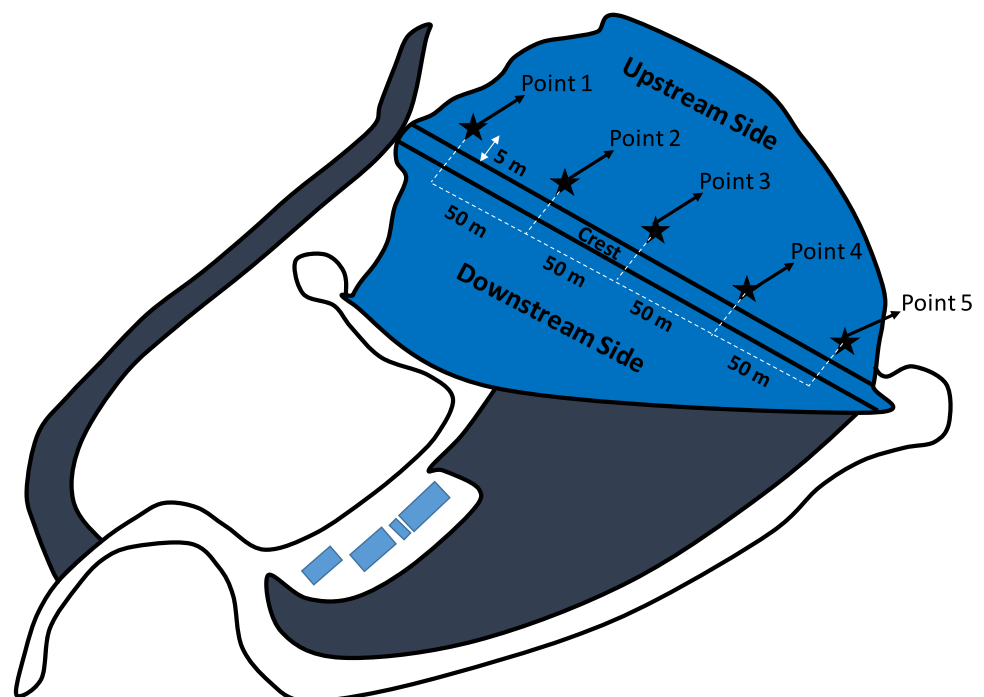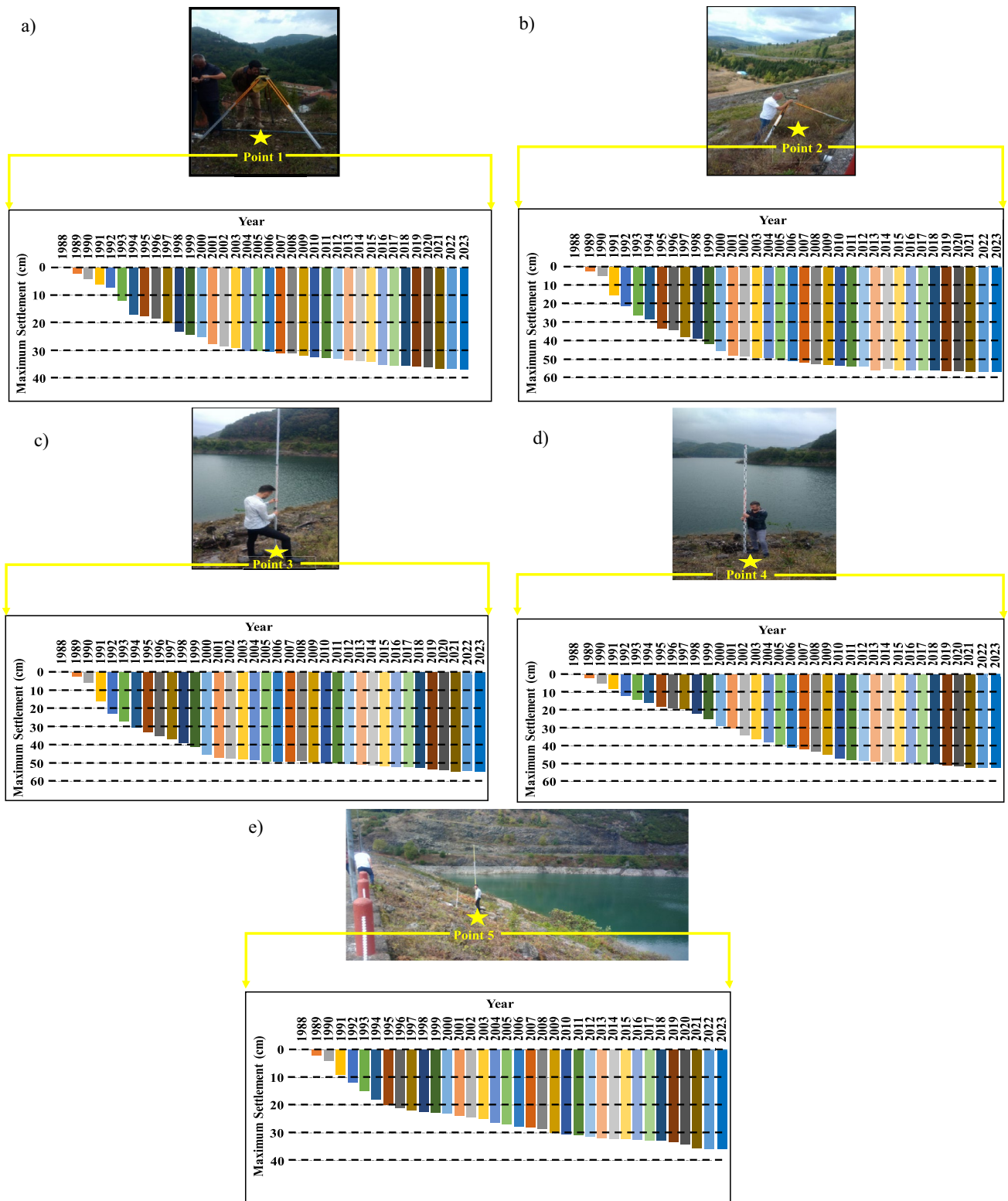
Fig. 6 Time-dependent settlement changes on five different points of the dam body

over 35 years. In 1989, the maximum settlement value on Point 2 was 2.17 cm, which increased to 14.4 cm by 1991, coinciding with the dam's maximum water level. While settlements continued to rise between 1989 and 2005, the rate of increase slowed after 2005. Notably, the largest settlement values on Point 2 were 51.2 cm in 2006 and 56.6 cm in 2023. Figure 6c presents time-dependent settlement changes for Point 3. From 1988 to 1989, a vertical displacement of 1.9 cm was observed on Point 3, with settlements escalating rapidly until 2001, reaching a maximum of 48.2 cm. By 2023, the maximum vertical displacement value on Point 3 had risen to 54.7 cm. Comparing settlement values on Points 2 and 3 over 35 years reveals the critical nature of the former. Settlements on Point 2 were more significant, indicating its heightened importance in understanding the time-dependent settlement behavior of clay core rockfill dams. Detailed vertical displacement values for Point 4 are presented in Fig. 6d. Within the first three years of impounding water, a total vertical displacement value of 11.7 cm was recorded on Point 4, reflecting the dam's rapid filling. While settlements increased swiftly until 2011, the rate of increase diminished significantly thereafter. Between 2011 and 2023, vertical

displacement values ranged from 48.3 to 52.07 cm. Similarly, Fig. 6e outlines the maximum vertical displacement values for Point 5. Between 1989 and 1991, these values ranged from 2.6 to 9.2 cm, increasing to 22.9 cm by 2000, significantly impacting both static and seismic behaviors. Although vertical displacements surged until 2008, the rate of increase declined notably afterward. By 2023, the maximum vertical displacement value on Point 5 had reached 35.7 cm. The time-dependent settlement results across all points provide vital insights into the settlement behaviors of clay core rockfill dams over 35 years. Notably, settlements on Point 2 emerged as the most critical, emphasizing its significance in understanding the time-dependent settlement behavior of such dams.

5 Three-dimensional modelling of Kozlu-Ulutan CCR Dam

The Kozlu-Ulutan Dam, recognized as one of the most significant clay core rockfill dams in the Black Sea region, was chosen for three-dimensional (3D) time-dependent

Fig. 7 View of blocks and 3D finite-difference model of Kozlu-Ulutan Dam
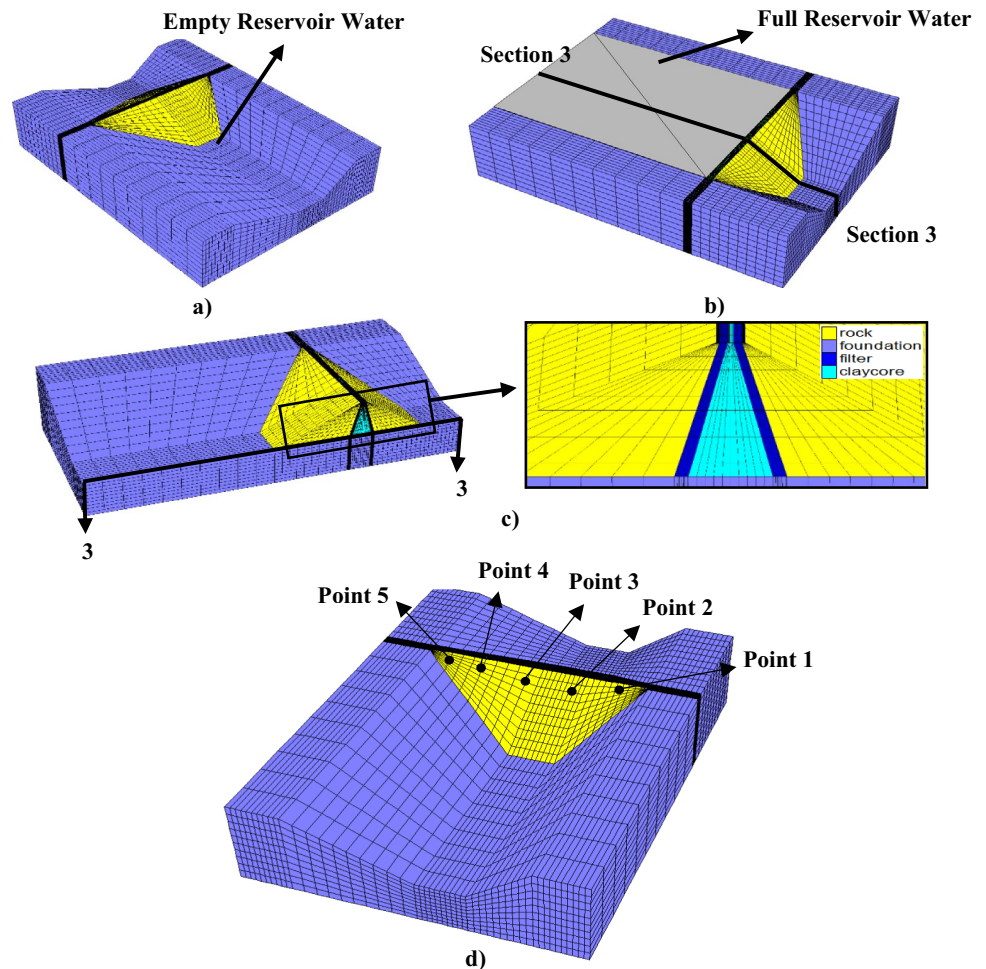
settlement and seismic analyses. FLAC3D software was utilized to create a detailed model and scrutinize the structural behavior of the dam. The 3D finite-difference model, featuring four distinct sections and three blocks, is depicted in Fig. 7. Rockfill materials and the foundation were modeled according to the original Kozlu-Ulutan dam project. The foundation was extended downstream and on the valley side to match the dam's height, while on the upstream side, it was extended to three times the dam's height. The foundation's height was also set equal to that of the dam. These dimensions were determined based on critical conditions for the reservoir water, dam body, downstream, and side sections, as outlined by Kartal et al. [24]. The 3D finite-difference model comprises a total of 1,304,547 finite-difference elements, with numerical analyses incorporating special material models for the dam's various components. Furthermore, interface elements [25] were employed to establish interaction conditions between the rockfill material-foundation and rockfill material-reservoir water. These elements (shear stiffness and normal stiffness) were considered as 10^8 Pa/m.

The Burger-Creep viscoplastic model was employed for both the rockfill materials and foundation to replicate the viscoplastic settlement behavior of dam body materials. This extensively used model has proven effective in simulating a broad spectrum of geotechnical engineering challenges, encompassing the behavior of tunnels, underground excavations, rock slope stability, and the performance of rock pillars in mines. Moreover, it has been instrumental in studying concrete behavior under loading conditions, offering engineers a framework to design structures that are not only safer but also more reliable. This viscoplastic model characterizes the time-dependent deformation behavior of rocks and similar materials, operating on the premise that deformation arises from the movement of dislocations within the crystal lattice of the material. Dislocations, being defects within the crystal structure, are capable of displacement under the influence of applied stress. Consequently, the movement of these dislocations leads to plastic deformation of the material. The Burger-Creep model delineates the deformation behavior into two distinct components: viscous and plastic. The former is associated with dislocation movement, while the latter corresponds to the creation and annihilation of dislocations. The strain rate, crucial in understanding the material's deformation, is governed by both viscous and plastic elements through a flow rule. This rule establishes a relationship between the strain rate, deviatoric stress, and an internal state variable that signifies the accumulation of plastic deformation. Over time, this internal state variable evolves, mirroring the accumulated plastic deformation. The strain rate evolution equation facilitates the update of the strain rate based on the prevailing stress conditions and the state of plastic deformation. To implement

the Burger-Creep model in FLAC3D, several parameters must be defined. These include the elastic modulus, Poisson's ratio, friction angle, and cohesion, which collectively delineate the material's elastic behavior. Additionally, parameters such as activation energy and diffusivity characterize the rate at which dislocations migrate within the crystal structure, while the grain size parameter influences the material's strength and deformation properties. Furthermore, the stress exponent and temperature exponent delineate the dependence of the deformation rate on applied stress and temperature. The deviatoric stress (S_{ij}) and strain (e_{ij}) components within this material model are computed as per the prescribed methodology [21].

$$S_{ij} = \sigma_{ij} - \sigma_0 \delta_{ij} \tag{1}$$

$$e_{ij} = \in_{ij} - \frac{e_{vol}}{3} \delta_{ij} \tag{2}$$

where

$$\sigma_0 = \frac{\sigma_{kk}}{3} \tag{3}$$

and

$$e_{vol} = \in_{kk} \tag{4}$$

Furthermore, the stresses and strains arising from the Kelvin, Maxwell, and plastic components are distinguished by the superscripts.K,.M, and.p, respectively. This notation allows for the description of the model's deviatoric behavior through the following equations:

Strain rate partitioning [21]:

$$e^{\bullet}_{ij} = e^{\bullet K}_{ij} + e^{\bullet M}_{ij} + e^{\bullet P}_{ij} \tag{5}$$

Kelvin:

$$S_{ij} = 2\eta^K e^{\bullet K}_{ij} + 2G^K e^{\bullet K}_{ij} \tag{6}$$

Maxwell:

$$e^{\bullet M}_{ij} = \frac{S^{\bullet}_{ij}}{2G^M} + \frac{S_{ij}}{2\eta^M} \tag{7}$$

Mohr–Coulomb:

$$e^{\bullet p}_{ij} = \lambda^* \frac{\partial g}{\partial \sigma_{ij}} - \frac{1}{3} e^{\bullet p}_{vol} \delta_{ij} \tag{8}$$

$$e^{\bullet p}_{vol} = \lambda^* \left[\frac{\partial g}{\partial \sigma_{11}} + \frac{\partial g}{\partial \sigma_{22}} + \frac{\partial g}{\partial \sigma_{33}} \right] \tag{9}$$

The volumetric response, on the other hand, can be expressed as [21]:

$$\sigma^{\bullet}_0 = K\left(e^{\bullet}_{vol} - e^{\bullet p}_{vol}\right) \tag{10}$$

The equations above pertain to the material characteristics of the bulk modulus K, shear modulus G, and dynamic viscosity η (kinematic viscosity multiplied by mass density). The Mohr–Coulomb model's yield envelope encompasses both tensile and shear criteria, and its yield condition is expressed as $f = 0$. When formulated in principal axes notation, the yield criteria take the form [21]:

Shear yielding [21]:

$$f = \sigma_1 - \sigma_3 N_\varphi + 2C\sqrt{N_\varphi} \tag{11}$$

Tension yielding [21]:

$$f = \sigma^t - \sigma_3 \tag{12}$$

The equation above consists of various parameters, including the cohesion C, the angle of internal friction φ, the tensile strength σt, and $N\varphi$, which is given by $(1 + \sin \varphi)/(1 - \sin \varphi)$. In addition, $\sigma 1$ and $\sigma 3$ denote the maximum and minimum principal stresses, with compression represented by negative values. The potential function g is formulated as [21]:

Shear failure [21]:

$$g = \sigma_1 - \sigma_3 N_\psi \tag{13}$$

Tension failure [21]:

$$g = -\sigma_3 \tag{14}$$

The expression provided above relates to the material dilation ψ, which is defined in terms of the parameter $N\psi$, given by $(1 + \sin \psi)/(1 - \sin \psi)$. It is important to note that the parameter $\lambda *$ is only active during plastic flow, and its value is determined by satisfying the plastic yield condition $f = 0$ [21]. The reservoir water was modeled considering the full reservoir water height of 64 m. Time-dependent results in creep analyses were obtained using specialized time codes available in the FLAC3D program. Through these specific time codes, the long-term creep behavior of the dam under study was derived in this research. Incorporating the influence of leakage on the viscoplastic behavior of the dam, the 3D model included the water table and hydrostatic water loads. Prior to commencing the finite-difference analyses, boundary movements of the 3D model were constrained. For settlement analyses, the bottom of the foundation was restricted in all three directions (x, y, z), while the side surfaces were permitted vertical movement (z) and restricted horizontal movement (x, y). To mitigate the reflection of earthquake waves from the lateral boundaries of the dam model, non-reflective boundary conditions were applied in the seismic analyses. Additionally, quiet boundary conditions were adopted for the lateral boundaries of the dam

model alongside free-field boundary conditions. The free-field (FF) boundary condition within the FLAC3D program is instrumental in minimizing wave reflections surrounding structures, particularly when modeling ground vibrations with horizontal and vertical components. It calculates wave propagation within a region encircling the simulation boundaries, known as the free field, thereby ensuring accurate results by simulating vibrations beyond the boundaries. Conversely, the quiet boundary condition relies on an artificial boundary designed to absorb incoming waves without reflecting them into the model. This is accomplished through a boundary layer comprised of synthetic materials, typically viscous dashpots, encircling the model perimeter. These dashpots effectively dampen waves, converting their energy into heat, thereby preventing reflections. Throughout the settlement and seismic analyses of the dam, the FLAC3D program encountered several errors, prompting the use of appropriate mesh intervals and numerous settlement analyses to ascertain the correct mesh intervals. Based on settlement analyses, a mesh width of 20 m was deemed suitable for settlement and seismic analyses of the Kozlu-Ulutan Dam.

6 Future seepage and settlement analysis results of Kozlu-Ulutan Dam

Monitoring the structural health of significant water structures like clay core rockfill dams is imperative for ensuring their long-term viability. This study specifically delved into the time-dependent settlement behavior of the Kozlu-Ulutan Dam, utilizing levelling measurements spanning 35 years alongside three-dimensional (3D) numerical modeling. Comparing the results of the 35-year settlement measurements with those of the 3D finite-difference analysis revealed a notable compatibility between the observation and analysis outcomes. Furthermore, a detailed analysis of the Kozlu-Ulutan dam's settlement behavior over the next 100 years (from 2023 to 2123) was conducted. Time-dependent settlement analyses furnished comprehensive insights into the dam's anticipated long-term settlement patterns. Future settlement analyses were executed by incorporating specialized time codes (fish codes) within the FLAC3D program. These time codes facilitated the estimation of the dam's settlement behavior under full reservoir conditions for the ensuing century. The procedural steps involved in conducting the future settlement analyses of the dam were meticulously outlined in Fig. 8. To obtain the future settlement behavior of the dam, specific time codes have been incorporated into the FLAC3D program, as indicated in Fig. 8. Through these time codes, the future settlement behavior of the dam can be simulated for the desired time. Time is defined in days within the
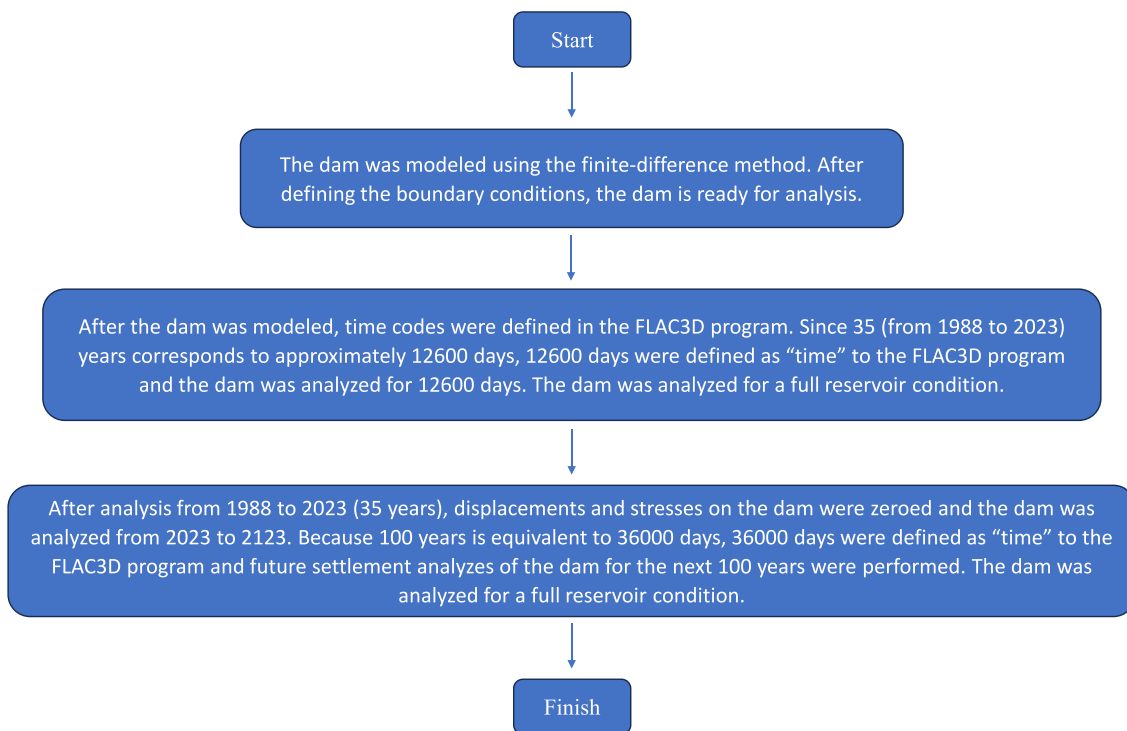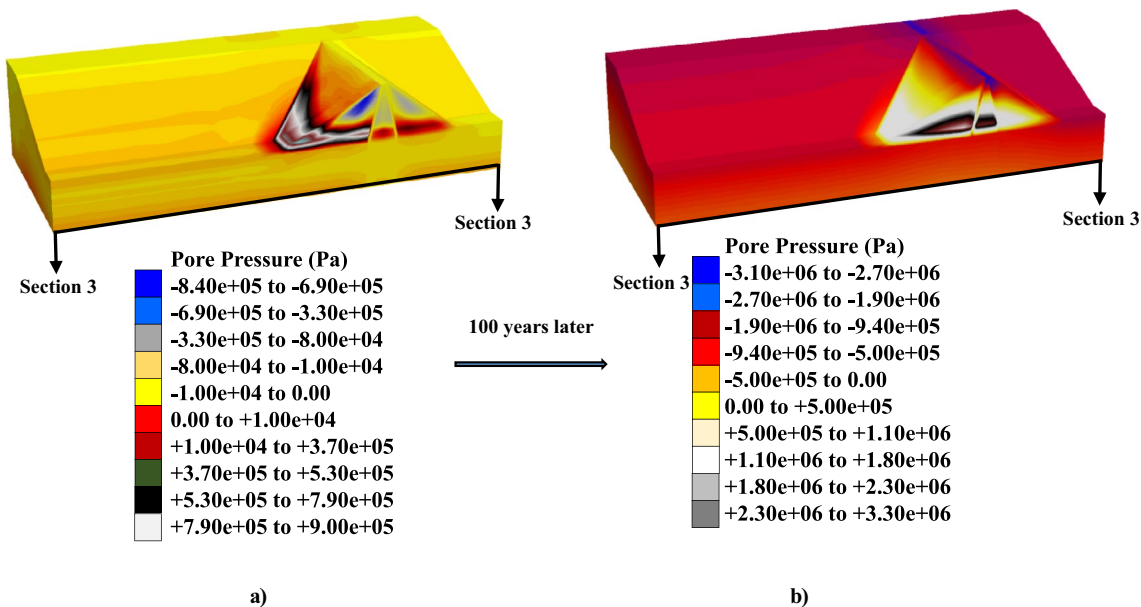
Fig. 8 Stages of future settlement analyses

Fig. 9 Seepage analysis results **a** current situation of the dam **b** future situation of the dam

program. Additionally, the resetting process mentioned in Fig. 8 is not the resetting of displacements and stresses obtained from 35 years of analysis, but rather a code written to observe the effects of 100 years of analysis on the dam. Through the resetting process, only displacement

values occurring in the dam body from its current state to 100 years ahead have been visualized.

In Fig. 9, the analysis initiates with seepage analyses conducted for both the present state and the anticipated condition of the dam over the next 100 years. These seepage

analyses were executed utilizing the "FLUID" module integrated into the FLAC3D program. Through this module, evolving pore pressure values within the dam body over time are depicted. While utilizing the FLUID module, the "fl" command was specified within the program, and the water table, representing the maximum dam level, was modeled at the upstream section of the dam body. Furthermore, specific fluid time codes were scripted and defined for both the present and the 100-year future conditions of the dam. To obtain seepage analysis results for the dam's condition projected 100 years ahead, a fluid time of 100 years was inputted into the program. These temporal codes unveil the time-dependent seepage behavior of the dam. The seepage behavior for both the present and the 100-year future conditions of the dam is illustrated in Fig. 9. According to Fig. 9, maximum pore pressures have manifested at the lower sections of the upstream part for the current state of the dam. Additionally, negligible pore pressures have been observed beneath the clay core. A detailed presentation of pore pressure values anticipated after 100 years within the dam body is depicted in Fig. 9b. As per Fig. 9b, significant

pore pressure values have been attained at the upstream side of the dam body. The maximum pore pressure value within the dam body is recorded as 3.3 MPa, indicating a substantial alteration in the dam's seepage behavior after 100 years when compared to its current state.

The time-dependent settlement analysis results for five different points on the dam body were depicted in Figs. 10, 11, 12, 13, 14. Figure 10 illustrated both levelling measurements and settlement analysis outcomes for Point 1, situated on the far right side of the dam body. A striking resemblance was observed between the levelling measurements and settlement analysis results. Figure 10b showcased three-dimensional settlement analyses of the dam spanning from 1988 to 2123. It indicated that the vertical displacements observed in the dam body from 1988 to 2023 aligned closely with the levelling measurements. Specifically, the largest displacement value at Point 1 in 2023 was recorded as 35.9 cm, whereas the projected maximum displacement value for Point 1 in 2123 was estimated to be 39 cm. Consequently, it could be inferred that after a century, there would be a 3.1 cm increase in
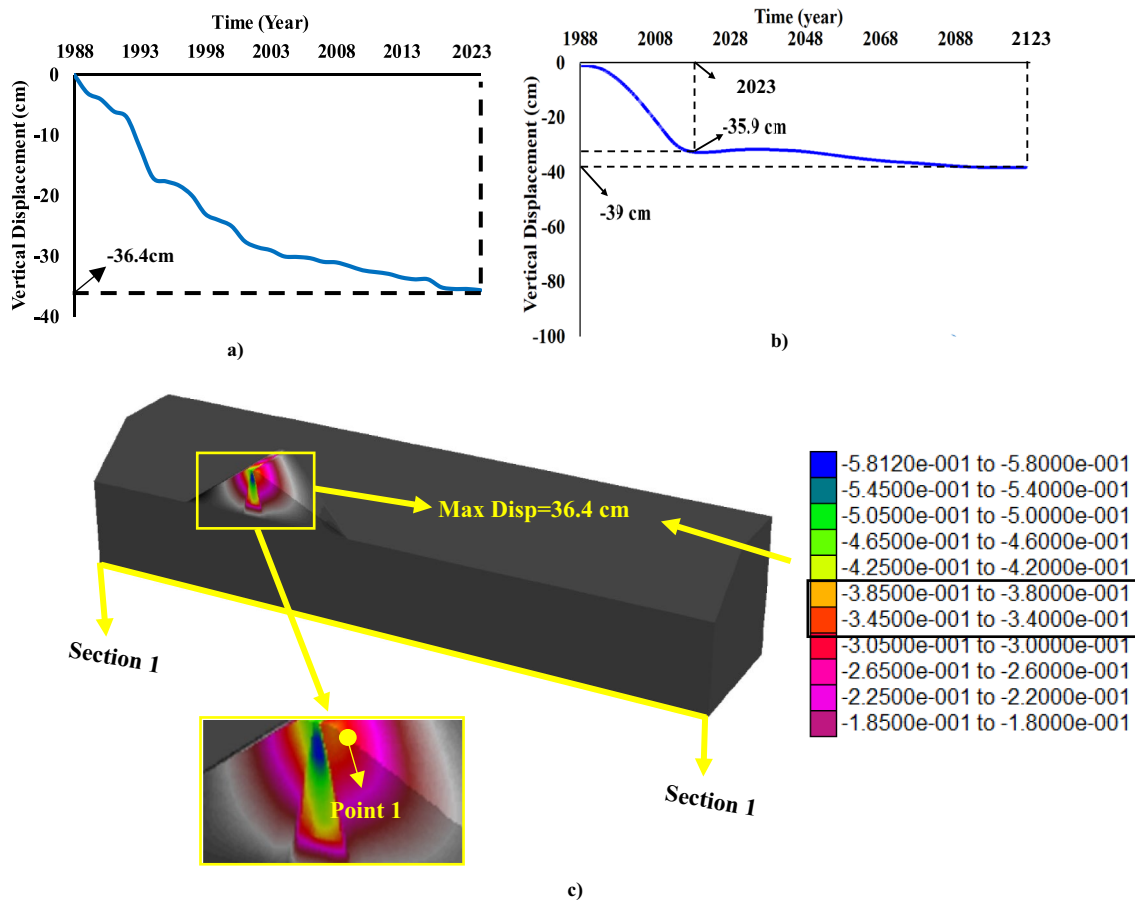

Fig. 10 Time-dependent settlement results on Point 1 **a** Levelling measurements for 35 years **b** 3D numerical observation for 135 years **c** Contour diagram of the dam in 2023
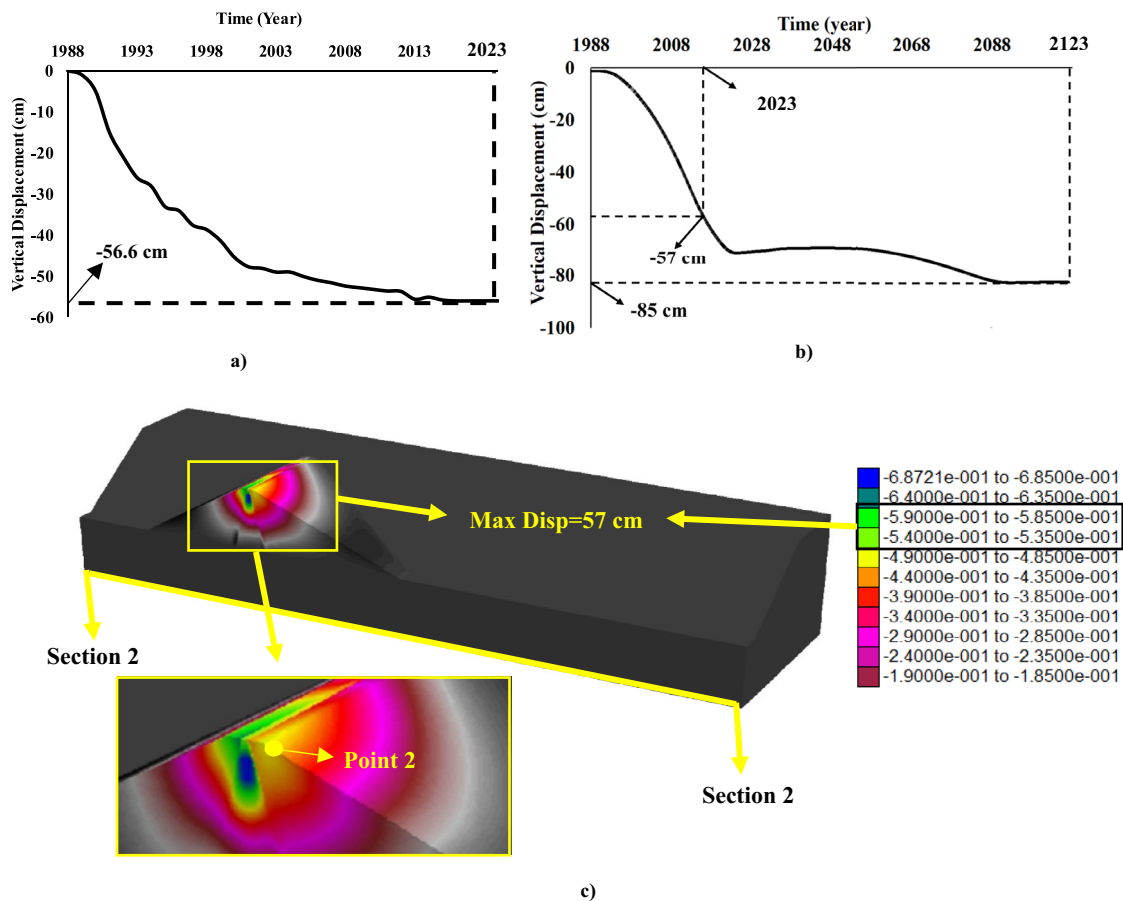
Fig. 11 Time-dependent settlement results on Point 2 **a** Levelling measurements for 35 years **b** 3D numerical observation for 135 years **c** Contour diagram of the dam in 2023

vertical displacement at Point 1 compared to the current state of the dam. This comprehensive insight contributed significantly to the literature regarding the prediction of future deformation behavior in clay core rockfill dams. Figure 10c displayed the three-dimensional finite-difference model of the dam, cut from Section 1–1 on the dam body, providing a more detailed observation of the vertical displacements occurring at Point 1 in 2023. Analysis of Fig. 10c revealed that the most substantial vertical displacements in the dam body transpired within the clay core. Additionally, a maximum vertical displacement of 40 cm was observed at Point 1 and its immediate surroundings. Figure 11 depicted the vertical displacement results occurring at Point 2 from 1988 to 2023, alongside detailed future settlement analysis outcomes. As illustrated in Fig. 11a, vertical displacement at Point 2 demonstrated continuous growth from 1988 to 2003, with a subsequent decrease in the rate of increase observed from 2003 to 2023, suggesting a gradual decline in vertical displacements within the dam body over time. In 2023, the maximum vertical displacement at Point 2 was recorded at

56.6 cm. Furthermore, the levelling measurement results (Fig. 11b) validated the three-dimensional settlement analysis findings, affirming a remarkable similarity between the settlement analysis and levelling measurement results.

According to Fig. 11b, it becomes apparent that by 2123, Point 2 will undergo a maximum displacement of 85 cm, signifying a 28.4 cm increase in vertical displacement compared to the current situation of the dam. This numerical finding offers researchers valuable insights into the potential future vertical displacement of CCR dams. Furthermore, future settlement analysis results of the dam reveal that the rate of increase in vertical displacements at Point 2 will gradually decrease over time. In Fig. 11c, the detailed 3D finite-difference model of the Kozlu-Ulutan dam, cut from Point 2, is showcased. Figure 11c indicates that in 2023, the most significant vertical displacements in the dam occurred within the clay core, with the highest displacements occurring at Point 2 and its surrounding areas, reaching approximately 60 cm. The crest section of the dam exhibited the largest displacements, while the lowest parts of the dam body displayed the smallest displacements. Additionally, it
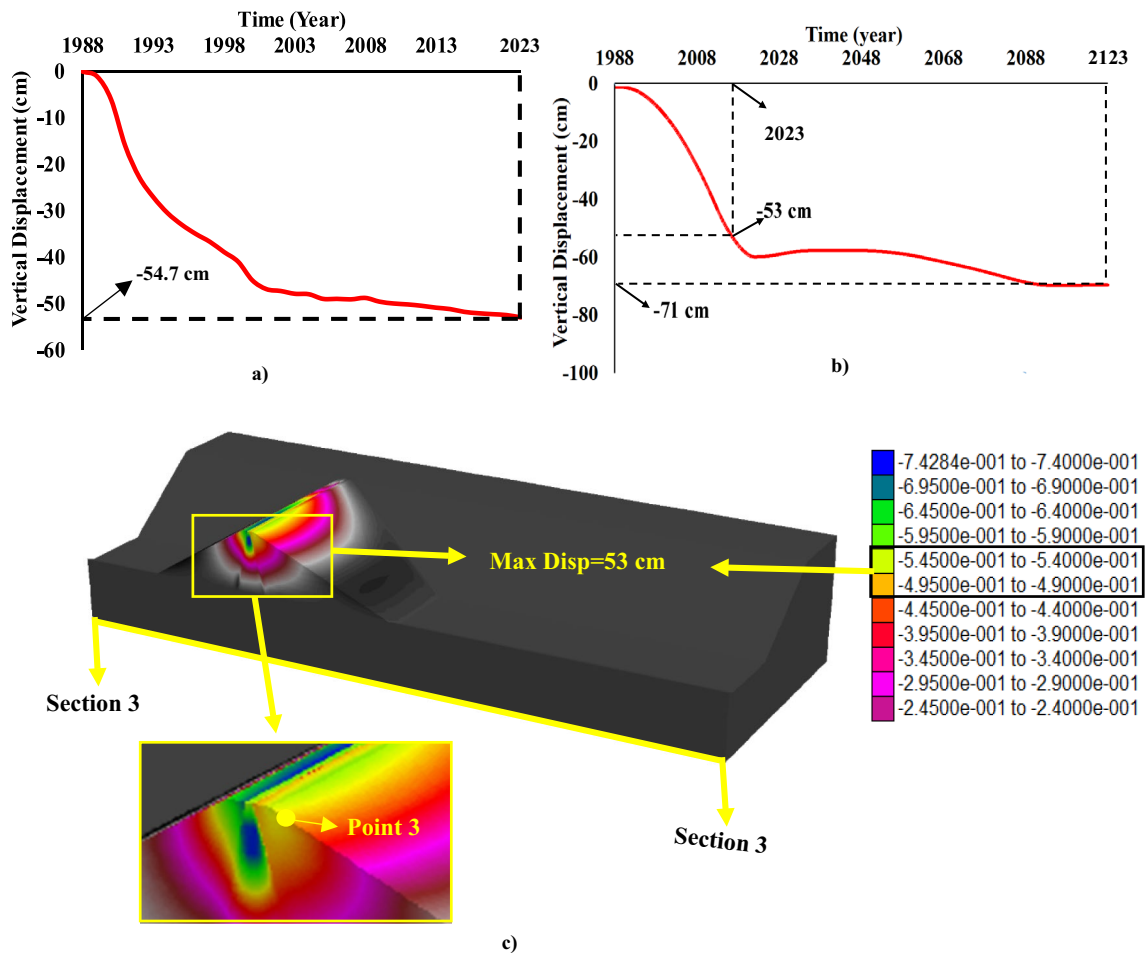
Fig. 12 Time-dependent settlement results on Point 3 **a** Levelling measurements for 35 years **b** 3D numerical observation for 135 years **c** Contour diagram of the dam in 2023

was observed that there were no vertical displacements in the foundation of the dam (Fig. 11c).

In Fig. 12, the vertical displacement results for Point 3 are presented based on both levelling measurements and three-dimensional settlement analyses. Figure 12a illustrates the graphical representation of vertical displacements at Point 3 over 35 years. A detailed examination of the levelling measurements reveals a continuous increase in the rate of vertical displacement at Point 3 from 1988 to 2001, followed by a subsequent decrease. This finding suggests a declining trend in the rate of vertical displacements within the clay core rockfill dam body over time. In 2023, the maximum vertical displacement at Point 3 was recorded as 54.71 cm. Figure 12b depicts the vertical displacement behaviors of the Kozlu-Ulutan Dam from 1988 to 2123, providing insights into the future vertical displacement patterns of the dam. According to Fig. 12b, the maximum displacement at Point 3 from 1988 to 2023 was 53 cm. Comparing this result with the levelling measurement findings suggests that the three-dimensional settlement analysis results corroborate the

levelling measurements. Moreover, it can be inferred that an additional 18 cm of vertical displacement is expected at Point 3 in the next 100 years. Figure 12c demonstrates that the most significant vertical displacements in the dam body occurred within the clay core. In Fig. 13, time-dependent vertical displacements at Point 4 are presented using both levelling measurements and settlement analyses. Figure 13a showcases the time-dependent vertical displacement results at Point 4 using levelling measurements. It shows that a maximum vertical displacement of 52.07 cm occurred at Point 4 between 1988 and 2023. Figure 13b presents detailed three-dimensional settlement analysis results for Point 4 from 1988 to 2123. It can be observed that the maximum vertical displacement reached at Point 4 in 2023 was 50.9 cm, a value similar to that obtained from levelling measurements in Fig. 13a. Moreover, the maximum vertical displacement expected to occur at Point 4 from 2023 to 2123 is 8.2 cm, indicating an additional 8.2 cm of vertical displacement is anticipated over the next 100 years of the dam's lifespan.
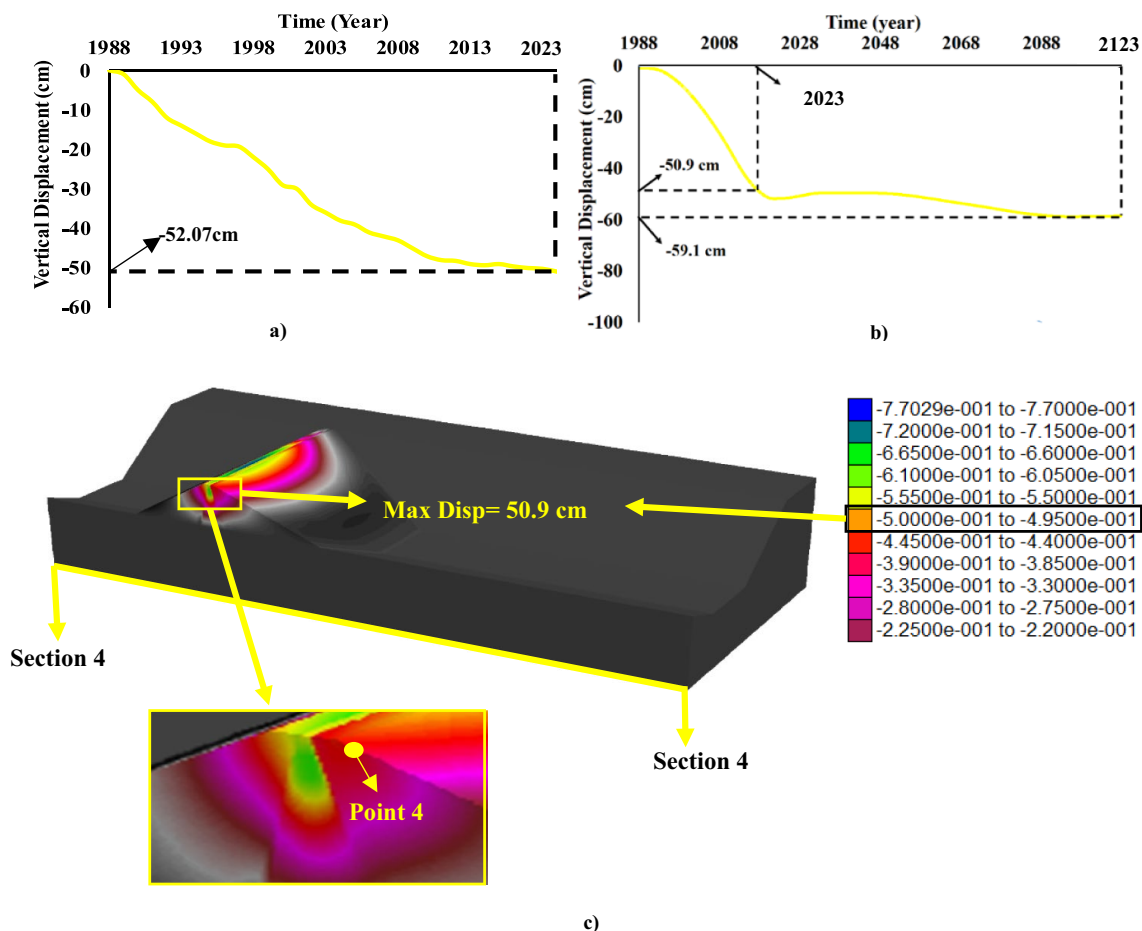
Fig. 13 Time-dependent settlement results on Point 4 **a** Levelling measurements for 35 years **b** 3D numerical observation for 135 years **c** Contour diagram of the dam in 2023

In Fig. 13c, a visualization of the dam's three-dimensional finite-difference model, divided into two, focusing on section Point 4, is presented. It is evident that the most significant vertical displacements occurred within the clay core of the dam. This finding underscores the critical importance of the clay core as a material component for CCR dams. Moving to Fig. 14, vertical displacements on Point 5 are depicted based on both levelling measurements and settlement analyses. According to the levelling measurement results, the maximum vertical displacement value on Point 5 from 1988 to 2023 is recorded as 35.71 cm, providing researchers with comprehensive insights into the long-term vertical displacement behavior of CCR dams. Figure 14b illustrates the time-dependent vertical displacement results on Point 5 from 1988 to 2123. The maximum vertical displacement on Point 5 from 1988 to 2023 was found to be 35.2 cm, a result consistent with the three-dimensional settlement analysis results. Moreover, the maximum vertical displacement expected to occur on Point 5 in 2123 is projected to be 38 cm. This outcome suggests that there will be

an additional 2.8 cm of vertical displacement on Point 5 of the Kozlu-Ulutan Dam over the next century.

7 Current and future seismic analysis results of Kozlu-Ulutan Dam

In this study, the Mohr–Coulomb material model was utilized for dynamic analyses, while the Burger-Creep material model was employed for creep analyses. This transition was necessitated by the fact that the material model tailored for creep analyses is exclusively suited for such analyses. Consequently, a change in material model was imperative when transitioning to dynamic analyses. The rockfill, filters, and core were characterized using the Mohr–Coulomb elasto-plastic model, which is recognized as a prominent failure model in soil mechanics. This model delineates failure conditions based on the fulfillment of the linear equation below, which relates shear stress (τ) and effective normal stress (σ') acting on any material element [8].
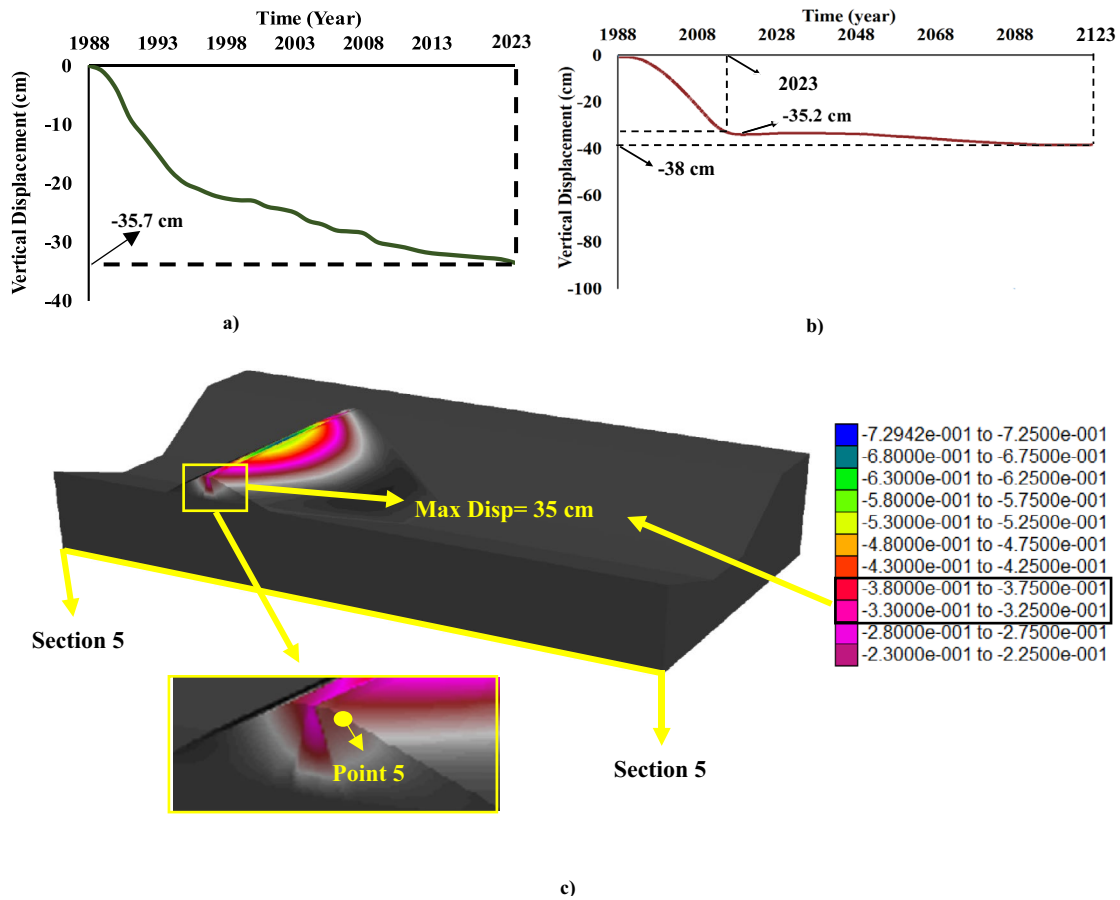
Fig. 14 Time-dependent settlement results on Point 5 **a** Levelling measurements for 35 years **b** 3D numerical observation for 135 years **c** Contour diagram of the dam in 2023

$$|\tau| = c + \sigma'\tan\phi \tag{15}$$

The parameters c and ϕ represent the cohesion and internal friction angle, respectively. When considering the principal effective stresses, Coulomb's yield criterion can be formulated using the subsequent Eqns. [8]:

$$f_{13} = \frac{(\sigma_1' - \sigma_3')}{2} - \frac{(\sigma_1' + \sigma_3')\sin\phi}{2} - c\cos\phi = 0 \tag{16}$$

$$f_{12} = \frac{(\sigma_1' - \sigma_2')}{2} - \frac{(\sigma_1' + \sigma_2')\sin\phi}{2} - c\cos\phi = 0 \tag{17}$$

$$\sigma_1' \geq \sigma_2' = \sigma_3' \tag{18}$$

The failure criterion can be reformulated in terms of deviatoric stress and mean effective stress, which is a more commonly used expression for delineating failure behavior in advanced soil models [8].

$$f_1 = q - \sin\phi(p' + c\cot\phi) \tag{19}$$

In the Mohr–Coulomb model, it is posited that the material exhibits elastic behavior until reaching the proximity of the failure surface. However, in actuality, plastic deformations initiate well before failure transpires. Nonetheless, this model persists in usage due to its simplicity and capacity to yield pragmatic solutions for significant geotechnical engineering challenges [8]. During the employment of this material model for dynamic analyses, the material parameters presented in Table 1 were utilized. After completing the time-dependent settlement analyses of the Kozlu-Ulutan Dam, the seismic analyses of the dam were thoroughly investigated. Seismic analyses involved the examination of 10 different earthquakes, chosen based on their significance as ground motions in Türkiye in 2023, which resulted in thousands of casualties. Figure 15 outlines the steps involved in seismic analyses for both the years 2023 and 2123. In this study, creep analyses were initially conducted, followed
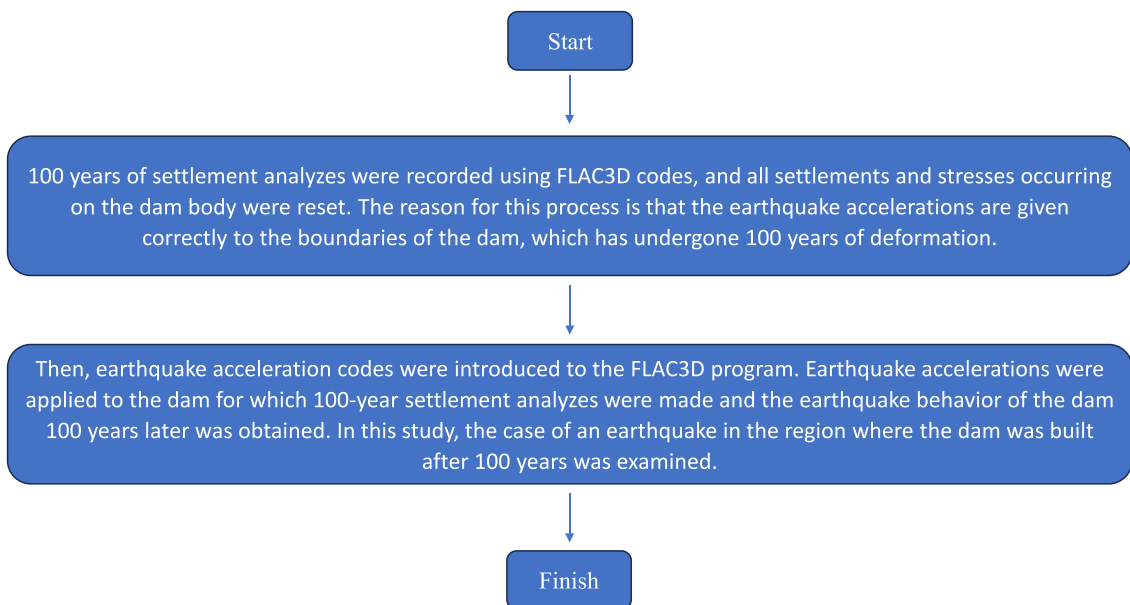
Start

100 years of settlement analyzes were recorded using FLAC3D codes, and all settlements and stresses occurring on the dam body were reset. The reason for this process is that the earthquake accelerations are given correctly to the boundaries of the dam, which has undergone 100 years of deformation.

Then, earthquake acceleration codes were introduced to the FLAC3D program. Earthquake accelerations were applied to the dam for which 100-year settlement analyzes were made and the earthquake behavior of the dam 100 years later was obtained. In this study, the case of an earthquake in the region where the dam was built after 100 years was examined.

Finish

Fig. 15 Stages of seismic analyses

by subjecting the dam, which had undergone creep analysis, to earthquake loads for seismic analyses. The "reset" operation, as indicated in Fig. 14, did not entail resetting the displacement and stress values occurring on the dam following the creep analysis. Instead, seismic accelerations were applied to the dam subsequent to the creep analyses, taking into account the stress and displacement values resulting from the creep analysis. However, as creep analysis results were presented in Sect. 6, Sect. 7 exclusively focuses on presenting the results of earthquake analyses. Thus, the reset process was solely utilized to exhibit earthquake analysis results, performed using the "ini" command. Seismic analyses were conducted considering the numerical results of the

dam, encompassing three-dimensional settlement analyses spanning 100 years (from 2023 to 2123). Initially, the settlements and stresses predicted to occur in 2123 were reset to accurately apply earthquake accelerations to the dam. This step ensured the correct application of earthquake accelerations to the deformed dam model in 2123, followed by obtaining earthquake analysis outcomes. Detailed insights into the future earthquake behavior of the dam were obtained as a result of the seismic analyses. Figure 16 displays the 3D seismic model of the dam, illustrating the free-field and quiet non-reflecting boundary conditions governing the boundary conditions of the 3D model. These boundary conditions aim to minimize the reflection of seismic waves propagating
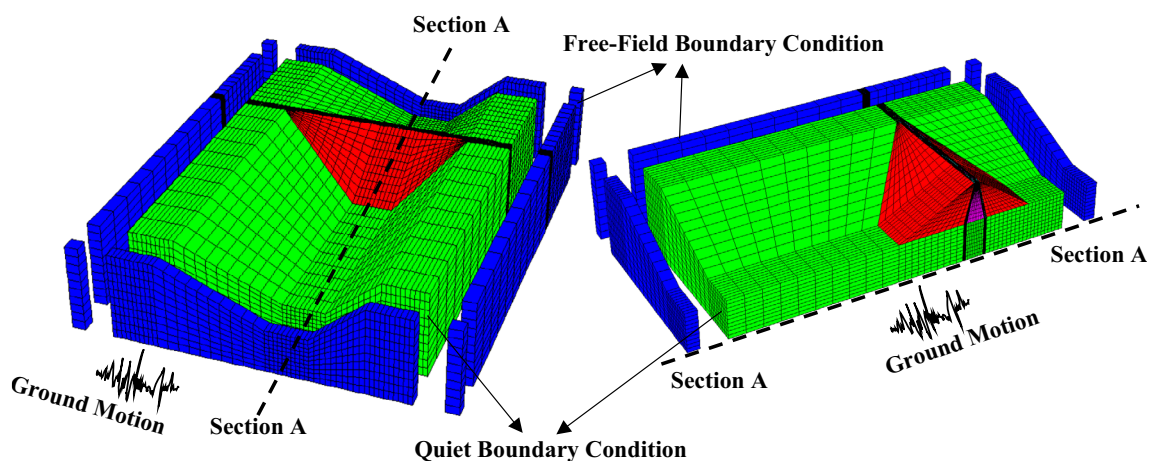

Fig. 16 Views of Kozlu-Ulutan Dams' three-dimensional seismic model and seismic boundary conditions

Table 2 Mechanical properties of strong ground motions [23]

Earthquake	Symbol	Year	M_w	Distance (km)	PGA (cm/s^2)	PGV (cm/s)	PGD (s)
Pazarcık1 (Kahramanmaraş)	EQ 1	2023	7.7	8.6	2178.72	212.94	262.17
Elbistan (Kahramanmaraş)	EQ 2		7.6	7	635.45	170.79	90.99
Nurdağı1 (Gaziantep)	EQ 3		6.6	6.2	454.15	44.60	214.37
Yayladağı (Hatay)	EQ 4		6.4	21.7	775.40	75.79	37.52
İslahiye (Gaziantep)	EQ 5		5.7	11.19	363.52	13.85	1.02
Yeşilyurt (Malatya)	EQ 6		5.6	6.15	24.31	1.22	0.48
Doğanşehir (Malatya)	EQ 7		5.6	10.23	47.28	2.90	0.40
Nurdağı2 (Gaziantep)	EQ 8		5.6	6.98	44.15	2.26	0.73
Pazarcık2 (Kahramanmaraş)	EQ 9		5.5	5.96	49.84	2.84	0.55
Ekinözü (Kahramanmaraş)	EQ 10		5.5	10.93	79.35	4.26	0.42

within the dam model from the model boundaries. Seismic accelerations were applied to the base of the foundation in the x, y, and z directions. Special fish functions and codes were employed to apply the seismic accelerations to the dam model. To better understand the seismic changes in the dam body, the dam body was cut from the A-A cross-section (Fig. 16).

The mechanical properties of the earthquakes utilized in the seismic analyses are outlined in Table 2. These earthquakes are notable events that have resulted in significant devastation in Türkiye. Specifically, the 2023 Kahramanmaraş Pazarcık (Mw: 7.7) and 2023 Kahramanmaraş Elbistan (Mw: 7.6) earthquakes, occurring with a mere 9-h interval, are considered rare occurrences with magnitudes exceeding 7. Given the Kozlu-Ulutan Dam's location along an active fault line, it is paramount to employ these earthquakes to scrutinize both the present and future seismic responses of the Kozlu-Ulutan Dam.

Figure 17 depicts the seismic displacement outcomes of the Kozlu-Ulutan Dam for EQ 1, EQ 2, EQ 3, and EQ 4 earthquakes. In Fig. 17a, it is notable that the seismic response of the dam analyzed under the EQ1 earthquake exhibited notable discrepancies between the years 2023 and 2123. Specifically, in 2023, a maximum displacement of 22 cm was observed in the lower section of the dam body, with an additional maximum displacement of 8 cm detected in the upstream segment. Moreover, the edge sections of the dam experienced a maximum displacement value of 10 cm. Conversely, in 2123, projections suggest a maximum displacement of 26 cm along the dam crest and an estimated maximum displacement of 14 cm at the base section of the dam (Fig. 17a). Concerning EQ2, Fig. 17b indicates a maximum displacement of 18 cm on the dam crest in 2023, with significant seismic displacement observed in both the upstream and downstream lower portions of the dam body. By 2123, it is anticipated that a maximum displacement of 20 cm will manifest in the middle section of the Kozlu-Ulutan Dam's upstream segment. Additionally, should the EQ1 earthquake occur in the vicinity of the dam's construction

site after 100 years, substantial seismic displacement values are expected to arise in the middle segments of the dam body (Fig. 17b).

These findings offer crucial insights into the future seismic behavior of the Kozlu-Ulutan Dam. For the EQ 3 earthquake, a peak displacement of 20 cm was recorded on the dam crest in 2023. In the middle section of the downstream part of the dam body, a maximum displacement of 6 cm was observed (Fig. 17c). It is predicted that by 2123, a maximum displacement of 24 cm will occur in the middle section of the dam's upstream portion (Fig. 17c). In comparison to the current state of the dam, an approximate additional settlement of 11 cm at the base of the dam body is estimated. Regarding the EQ4 earthquake, in 2023, maximum displacements of approximately 14 cm occurred between the downstream and crest sections of the dam body (Fig. 17d). Additionally, if the same earthquake recurs in the Kozlu-Ulutan Dam after 100 years, it is anticipated that 18 cm more settlement will take place on the dam crest. Figure 18 provides a detailed overview of the seismic behavior of the Kozlu-Ulutan Dam for EQ 5, EQ 6, EQ 7, and EQ 8 earthquakes. In 2023, a maximum settlement value of 21 cm was obtained on the crest region of the dam. In the base sections of the dam, a maximum vertical displacement value of approximately 8 cm was recorded. This underscores the criticality of the upper portions of the dam during earthquakes. For EQ6 earthquake, a maximum displacement of 18 cm was observed around Point 2 in 2023 (Fig. 18b), with 13 cm maximum displacement occurring in the downstream section of the dam. Predictions for 2123 suggest a vertical displacement value of 20 cm in the middle section of the dam's upstream portion. Figure 18c illustrates the seismic displacement behavior of the Kozlu-Ulutan dam for the EQ7 earthquake, showing a maximum displacement value of 22 cm on the crest region of the dam in 2023. Lower displacement values were observed in the downstream section of the dam compared to the upstream portion. It is predicted that 24 cm more vertical displacement will occur
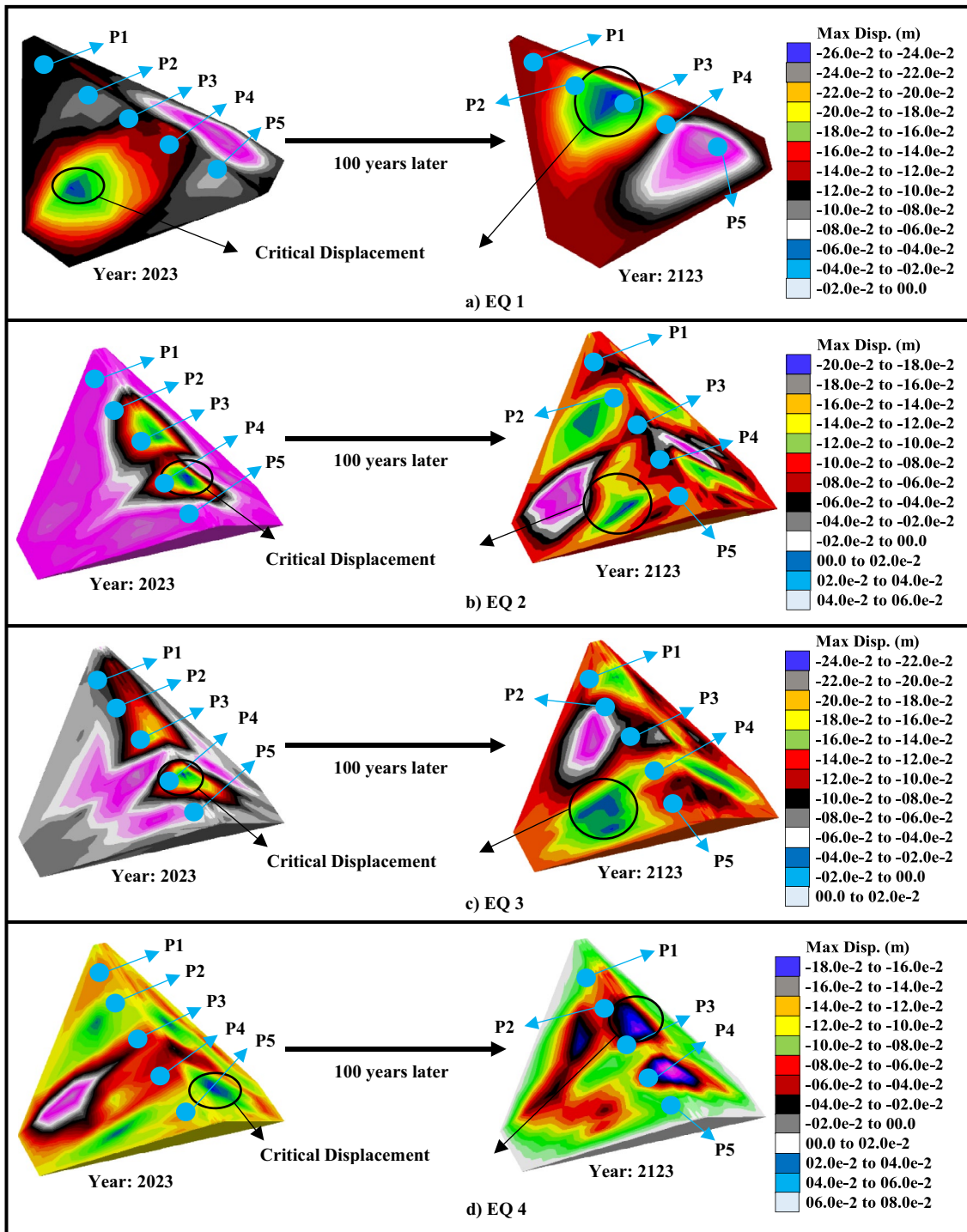
Fig. 17 Maximum seismic displacement results of Kozlu-Ulutan dam for EQ 1, EQ 2, EQ 3, and EQ 4 earthquakes

in the upstream portion of the dam by 2123. For the EQ8 earthquake, a maximum displacement of 17 cm occurred on the crest of the Kozlu-Ulutan Dam in 2023. In 2123, it is predicted that a maximum displacement value of 18 cm will take place in the middle sections of the dam's upstream and downstream portions (Fig. 18d). Regarding

the EQ 9 earthquake, in 2023, a maximum displacement of 25 cm was recorded on the crest of the Kozlu-Ulutan dam. In 2123, it is anticipated that a maximum displacement value of 26 cm will happen in the base section of the dam's upstream portion and the middle section of the downstream portion (Fig. 19a). For the EQ10 earthquake,
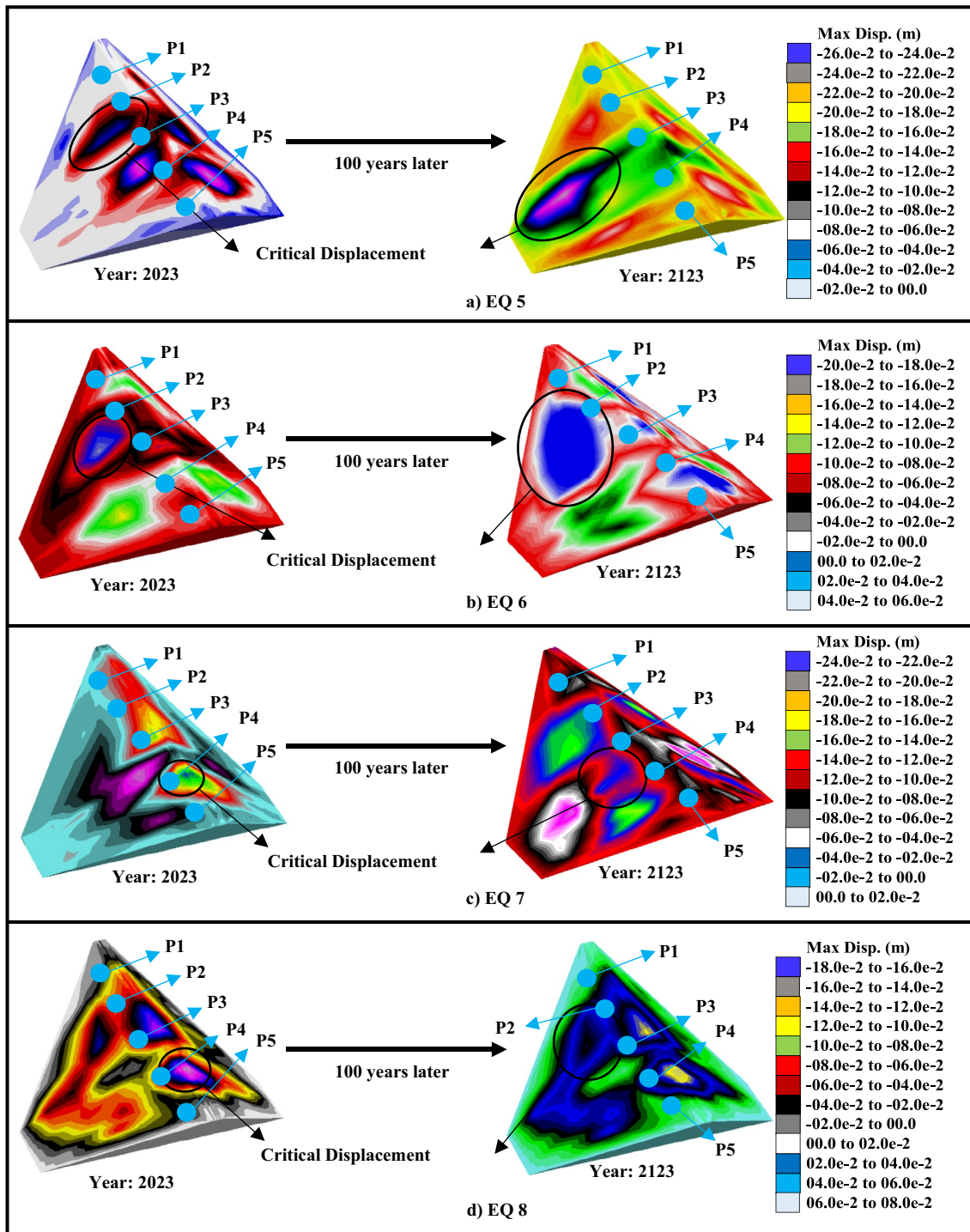
Fig. 18 Maximum seismic displacement results of Kozlu-Ulutan dam for EQ 5, EQ 6, EQ 7, and EQ 8 earthquakes

in 2123, it is predicted that approximately 20 cm maximum displacement will occur in the crest and upstream sections of the dam (Fig. 19b).

Figure 20 illustrates the seismic principal stress results on the Kozlu-Ulutan dam body for EQ 1, EQ 2, EQ 3, and EQ 4 earthquakes. The dam model was analyzed from Point 2, displaying the time-dependent principal stress values. In Fig. 20a, principal stress values for the EQ1 earthquake show a maximum value of approximately 5.8 MPa at Point 2 in 2023, with significant values observed in the dam body filters. Additionally, a maximum value of 5.6 MPa was noted at the base of the dam's upstream section. By 2123, it is
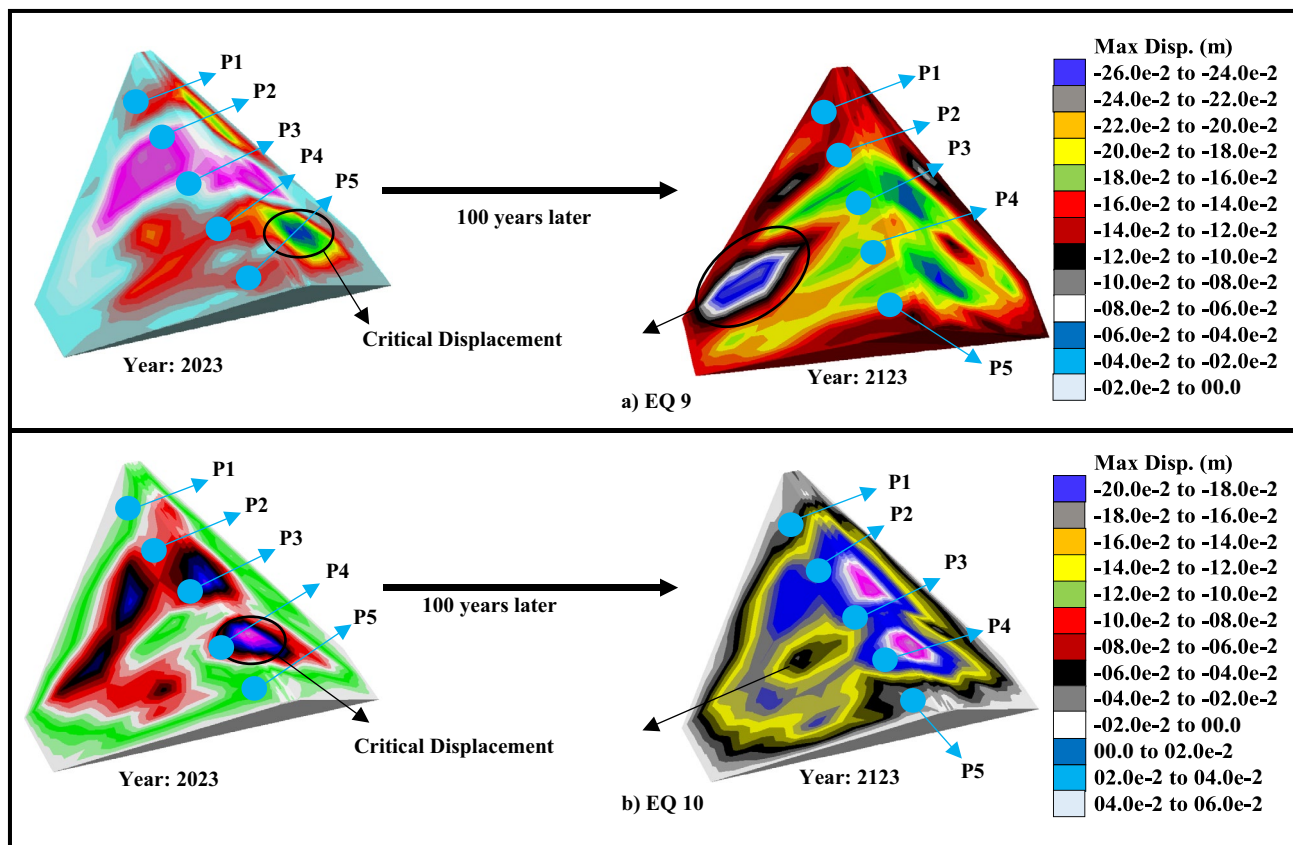
Fig. 19 Maximum seismic displacement results of Kozlu-Ulutan dam for EQ 9 and EQ 10 earthquakes

predicted that a maximum principal stress value of 11.8 MPa will occur at Point 2, with significant stress values expected in the rockfill material and filter zones of the dam. For the EQ2 earthquake (Fig. 20b), a maximum principal stress of 3.6 MPa was observed on Point 2 in 2023, with a maximum stress value of 2.1 MPa in the middle section of the dam's upstream portion. By 2123, a maximum principal stress value of 9.7 MPa is predicted at Point 2, indicating surface areas of the dam being more critical than the inner parts. Figure 20c shows results for the EQ3 earthquake, with a maximum principal stress value of 2.7 MPa observed at Point 2 in 2023. By 2123, a maximum stress value of 8.5 MPa is predicted at Point 2, with significant values expected in the clay core and filter sections of the dam. For the EQ4 earthquake (Fig. 20d), a maximum principal stress value of approximately 2.8 MPa was obtained on Point 2 in 2023. By 2123, a maximum principal stress value of 5.6 MPa is predicted at Point 2, with significant stress values expected in the rockfill material of the dam's upstream section. Figure 21 evaluates the seismic principal stress behavior of the Kozlu-Ulutan Dam for the EQ 5, EQ 6, EQ 7, and EQ 8 earthquakes. For the EQ5 earthquake, a maximum principal stress value of approximately 5.7 MPa was observed at Point 2 in 2023, with 3.1 MPa maximum principal stress at the

base of the clay core. By 2123, a maximum principal stress value of 9.8 MPa is predicted at Point 2, indicating larger principal stresses in the upstream and downstream sections of the dam compared to the current state.

Additionally, it is believed that after 100 years, greater stress values will occur on the surface of the dam body compared to the inner parts. For the EQ 2 earthquake, a maximum principal stress value of 5.4 MPa was observed at Point 2 in 2023. In the dam body filters, the maximum stress of 11.2 MPa was obtained, while a 6.2 MPa maximum principal stress value was observed on the rockfill material. For the year 2123, a maximum stress value of 11.6 MPa was predicted at Point 2. It is expected that smaller principal stress values will occur in the downstream section of the dam compared to the upstream section (Fig. 21b). Figure 21c presents the time-dependent principal stress values occurring at Point 2 during the EQ 7 earthquake. In 2023, the maximum stress value observed at Point 2 is 3.6 MPa, with a maximum stress value of 7.2 MPa observed in the dam body filters. Critical stress values were observed in the clay core of the dam. For 2123, it is predicted that a maximum principal stress value of 7.4 MPa will occur at Point 2. Moreover, a maximum stress value of 7.1 MPa is anticipated at the base of the downstream section of the dam
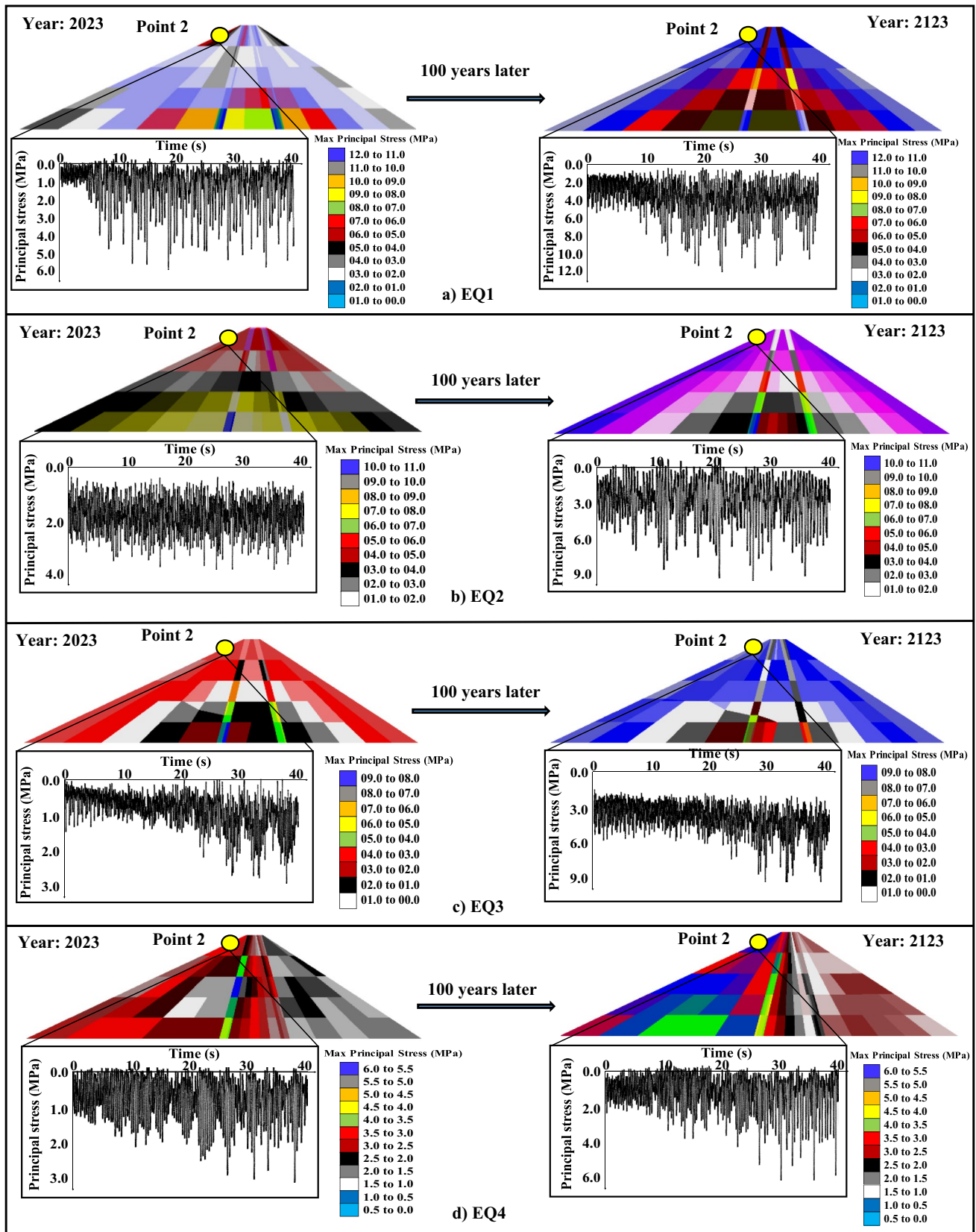
Fig. 20 Maximum principal stress results on the Kozlu-Ulutan dam for EQ 1, EQ 2, EQ 3, and EQ 4 earthquakes
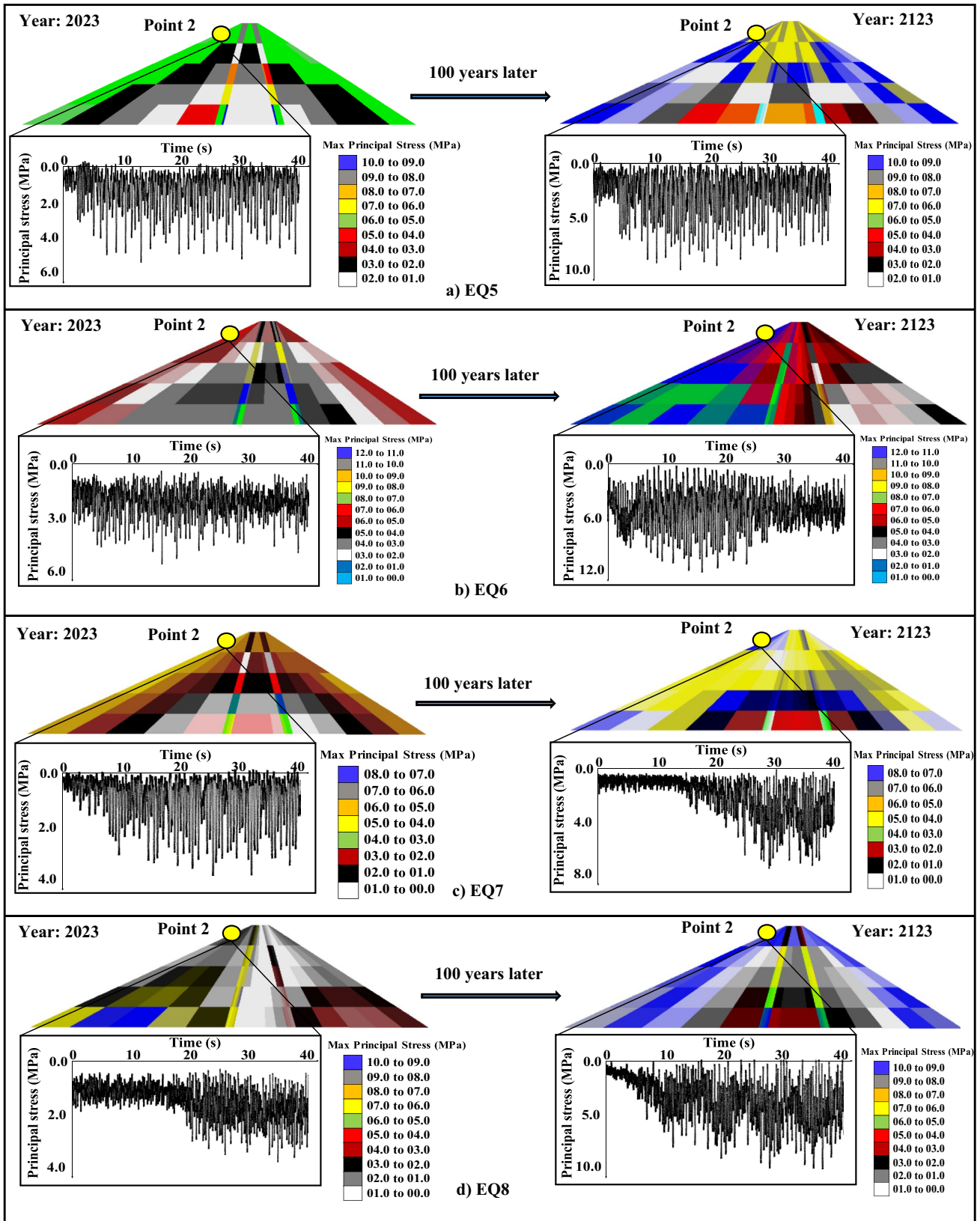
Fig. 21 Maximum principal stress results on the Kozlu-Ulutan dam for EQ 5, EQ 6, EQ 7, and EQ 8 earthquakes
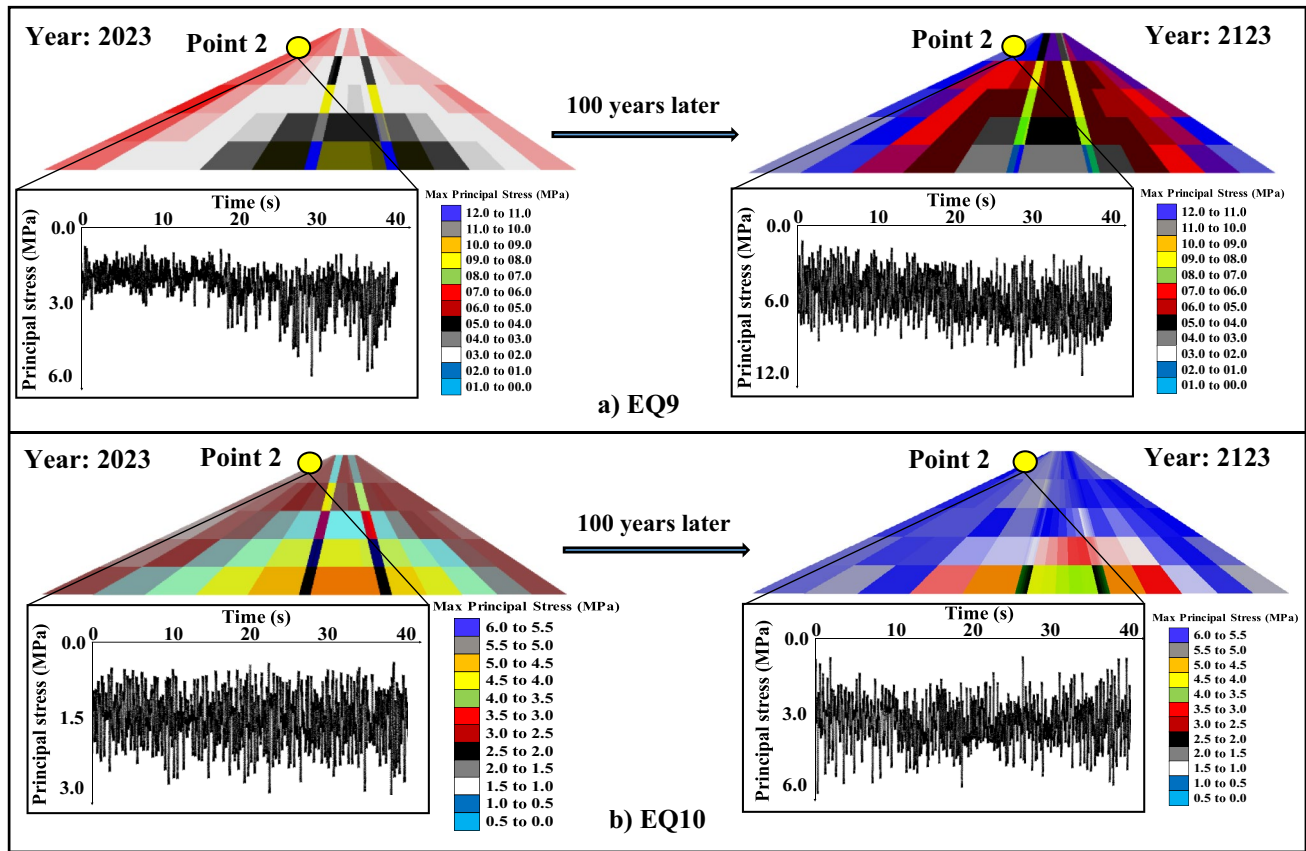
Fig. 22 Maximum principal stress results on the Kozlu-Ulutan dam for EQ 9 and EQ 10 earthquakes

body. Additionally, significant stress values are expected at the base of the clay core (Fig. 21c). For the EQ 8 earthquake, the largest principal stress value observed at Point 2 is approximately 3.5 MPa in 2023. Critical stress values that could affect dam safety were observed at the base of the upstream section of the dam. The maximum stress value of 2.8 MPa was obtained in the clay core of the dam. For 2123, it is believed that a maximum stress value of 7.1 MPa will occur in the dam body filters. Additionally, significant stress values are estimated to occur on the downstream and upstream surfaces of the dam (Fig. 21d). Figure 22 illustrates the seismic principal stress behavior of the Kozlu-Ulutan Dam for the EQ 9 and EQ 10 earthquakes. For the EQ 9 earthquake, the largest principal stress value observed at Point 2 is approximately 5.2 MPa in 2023. Additionally, a maximum stress value of 10.9 MPa was observed in the dam body filter material, while at the base of the clay core, a maximum stress value of 6.6 MPa is obtained (Fig. 22a). In 2123, it is predicted that the largest stress value occurring at Point 2 will be approximately 11.7 MPa, with an expected maximum stress value of 11.1 MPa in the filter material. For the EQ10 earthquake, it is projected that in the years 2023 and 2123, Point 2 will experience maximum principal stress values of 2.6 MPa and 5.9 MPa, respectively. Furthermore,

in 2023, a maximum stress value of 3.2 MPa was obtained on the base of the dam body's filter material. In 2123, significant stress values are anticipated to occur in the upstream and downstream sections of the rockfill material (Fig. 22b).

The seismic damage analysis results presented in Figs. 23 and 24 provide crucial insights into the anticipated behavior of the Kozlu-Ulutan Dam under various earthquake scenarios for both the years 2023 and 2123. These findings underscore the importance of understanding the evolving seismic vulnerabilities of the dam over time, especially with respect to shear and tension damages. In the analysis for 2023, it was observed that tension and shear damages were predominantly concentrated in the base region and rockfill material of the dam. However, for the year 2123, significant shear damages are expected to occur around the clay core and filter materials, indicating a shift in the distribution of damages over time. Notably, specific earthquakes such as EQ 2, EQ 5, EQ 6, EQ 8, and EQ 10 exhibited varying degrees of shear and tension damages in different sections of the dam in both 2023 and 2123. These observations highlight the complex and dynamic nature of seismic response in the dam structure and emphasize the need for continuous monitoring and adaptation to mitigate potential risks. Overall, these
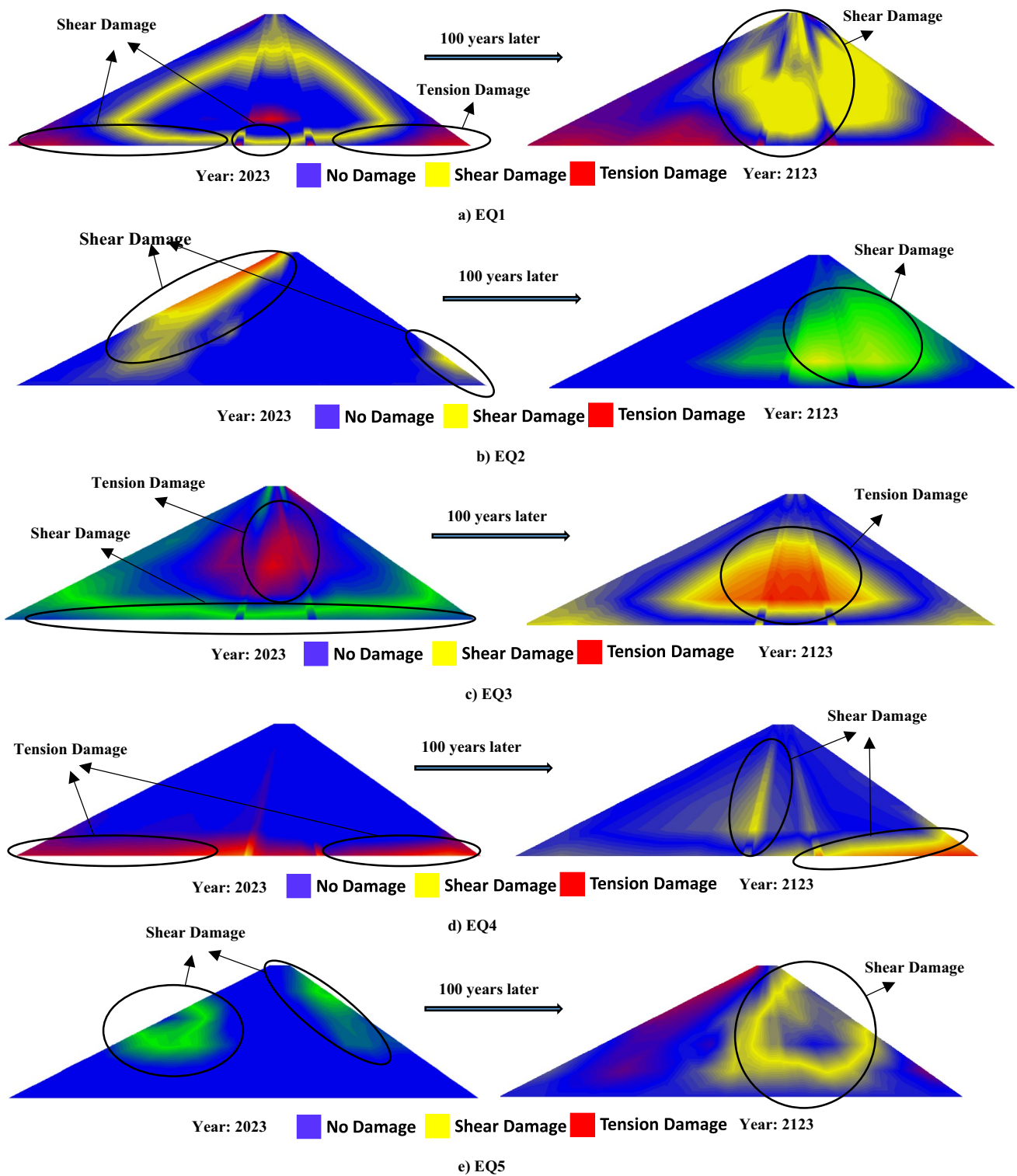
Fig. 23 Seismic damage performances of Kozlu-Ulutan dam for EQ 1, EQ 2, EQ 3, EQ 4, and EQ 5 earthquakes

findings offer valuable insights into the evolving seismic damage behaviors of clay core rockfill dams and underscore the importance of proactive measures to ensure the long-term safety and stability of such structures.

8 Conclusions

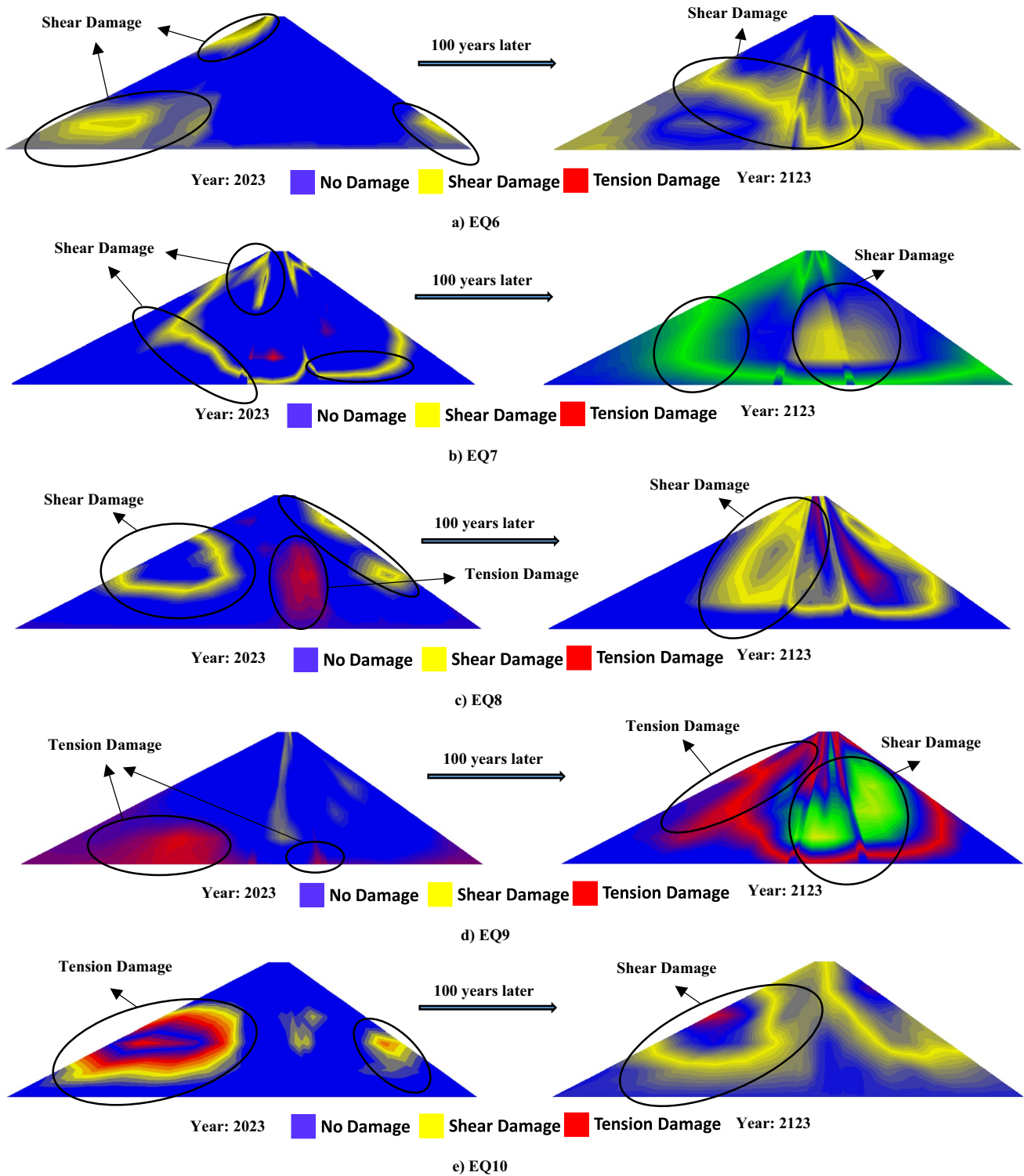Monitoring the structural integrity of water structures, particularly clay core rockfill dams is crucial for their long-term

Fig. 24 Seismic damage performances of Kozlu-Ulutan dam for EQ 6, EQ 7, EQ 8, EQ 9, and EQ 10 earthquakes

sustainability. This study verified the time-dependent settlement behavior of the Kozlu-Ulutan Dam through 35 years of levelling measurements. In addition, predictions for the dam's settlement behavior over the next 100 years were performed based on these measurements. Then, the current and future seismic behaviors of the dam were examined under 10 different strong ground motions. The study revealed the following significant results:

The 35-year levelling measurements revealed that Point 2 experienced the largest vertical displacements, while the edges of the dam body exhibited the smallest displacements. Notably, vertical displacements on Point 2 increased rapidly from 1988 to 2005 but slowed down after 2005.

The 35-year levelling measurements with 3D settlement analysis results demonstrated a high level of similarity along all points of the dam body. This result shows that the chosen material model, boundary conditions, and mesh intervals for the 3D settlement analysis were appropriate. Consequently, the material model, boundary conditions, and mesh intervals used for the settlement analysis of the Kozlu-Ulutan clay core rockfill dam are recommended for similar analyses of other clay core rockfill dams.

Future vertical displacement analyses were made for the dam and it was projected that after 100 years, Point 1 would experience an additional 3.1 cm of vertical displacement, and Point 2 would undergo an increase of 28.4 cm compared to the current situation. As a result, an approximate 49.12% increase in vertical displacement on Point 2 is expected in 2123 compared to 2023. Vertical displacements on Point 2 are predicted to continue increasing until 2025, followed by a significant reduction in the increase rate of displacement until 2123.

The seismic analyses showed that greater vertical displacements will be on the dam body in 2123 as compared to 2023. Higher seismic displacement values were observed in the filter and clay core materials of the dam for the years of 2023 and 2123, surpassing those in other parts of the dam.

Based on the seismic analysis results, it was concluded that the seismic stress values on the dam body in 2123 will be approximately twice as large as those in 2023. This finding indicates that the structural deteriorations occurring until 2123 will have a substantial impact on the dam's seismic behavior. Besides, the seismic damage analyses of the Kozlu-Ulutan dam after 100 years showed that significant seismic shear and tension damages in the clay core and filter materials of the dam will occur. These findings provide valuable insights into the future damage behavior of the dam.

Data availability The authors confirm that the data supporting the findings of this study are available within the article. The data that support the findings of this study are available from the corresponding author upon reasonable request.

Declarations

Conflict of interest The authors declare that they have no known competing financial interests or personal relationships that could have appeared to influence the work reported in this study.

Ethical approval This article does not contain any studies with human participants or animals performed by any of the authors.

References

1. Cetin H, Alizadeh M, Ertunç A (2000) Settlement and slaking problems in the world's fourth largest rock-fill dam, the Ataturk Dam in Türkiye. Eng Geol 56:225–242
2. Mahinroosta R, Alizadeh A, Gatmiri B (2015) Simulation of collapse settlement of first filling in a high rockfill dam. Eng Geol 187:32–44
3. Liu Sh, Lj W, Zj W, Bauer E (2016) Numerical stress-deformation analysis of cut-off wall in clay-core rockfill dam on thick overburden. Water Sci Eng 9:219–226
4. Neves EMd, Pinto AV (1988) Modelling collapse on rockfill dams. Comput Geotech 6:131–153
5. Habibagahi G (2002) Post-construction settlement of rockfill dams analyzed via adaptive network-based fuzzy inference systems. Comput Geotech 29:211–233
6. Haeri SM, Faghihi D (2009) A comparison between monitoring and analysis of Taleghan rockfill dam during construction. Proceedings of the 17th international conference on soil mechanics and geotechnical engineering 3: 2088–2091.
7. Dolezalova M, Hladik I (2011) Long-term behavior and safety assessment of Sance rockfill dam. Front Archit Civil Eng China 5:79–89
8. Rashidi M, Haeri SM (2017) Evaluation of behaviors of earth and rockfill dams during construction and initial impounding using instrumentation data and numerical modelling. J Rock Mech Geotech Eng 9:709–725
9. Wei K, Chen S, Li G, Han H (2022) Application of a generalised plasticity model in high earth core dam static and dynamic analysis. Eur J Environ Civ Eng 24:979–1012
10. Pinyol NM, Alonso EE (2019) Design, construction, monitoring and modelling of Albagés earth dam: a case history. Int J Civil Eng 17:501–513
11. Liu S, He W, Sun Y, Shen C, Wang L (2023) Analysis of the behavior of a high earth-core rockfill dam considering particle breakage. Comput Geotech 157:105320

12. Feng W, Chi S, Jia Y (2023) Random finite element analysis of a clay-core-wall rockfill dam considering three-dimensional conditional random fields of soil parameters. Comput Geotech 159:105437

13. Li Y, Min K, Zhang Y, Wen L (2023) Prediction of the failure point settlement in rockfill dams based on spatial-temporal data and multiple-monitoring-point models. Eng Struct 243:112658

14. Chen Z, Yin Y, Yu J, Cheng X, Zhang D, Li Q (2022) Internal deformation monitoring for earth-rockfill dam via high-precision flexible pipeline measurements. Autom Constr 136:104177

15. Chen Y, Lin G, Lu Y (2022) Deformation and stability analysis of a core rockfill dam with leakage. Shock Vib 2022:6944442

16. Costigliola RM, Mancuso C, Pagano L, Silvestri F (2022) Prediction of permanent settlements of an upstream faced earth dam. Comput Geotech 144:104594

17. Guan Z, Sun X, Zhang G, Li G, Huang P, Zhang B, Wang J, Zhou X (2022) Deformation and damage behavior of the deep concrete cut-off wall in core earth-rock dam foundation based on plastic damage model - a case study. Structures 46:1480–1494

18. Xu M, Jin D, Song E, Shen Z, Yang Z, Fu J (2019) Full-scale settlement test and back-analysis of the long-term settlement of heavy-loaded shallow foundations on a high rockfill embankment. Comput Geotech 115:103156

19. Yao F-h, Guan S-h, Yang H, Chen Y, Qiu H-f, Ma G, Liu Q-w (2019) Long-term deformation analysis of Shuibuya concrete face rockfill dam based on response surface method and improved genetic algorithm. Water Sci Eng 12:196–204

20. Sukkarak R, Jongpradist P, Pramthawee P (2019) A modified valley shape factor for the estimation of rockfill dam settlement. Comput Geotech 108:244–256

21. Itasca (2002) Inc. FLAC version 5 user manual. Minneapolis, USA: Itasca Consulting Group, Inc.

22. DSI (2023) General directorate of state hydraulic works, regional directorate, Zonguldak, Turkey.

23. AFAD (2023) Disaster and emergency management presidency.

24. Kartal ME, Cavusli M, Sunbul AB (2017) Assessing seismic response of a 2D roller-compacted concrete dam under variable reservoir lengths. Arab J Geosci 10:488

25. Ouzandja D, Tiliouine B (2015) Effects of dam-foundation contact conditions on seismic performance of concrete gravity dams. Arab J Sci Eng 40:3047–3056

26. Zhang H, Jing Y, Chen J, Gao Z, Xu Y (2022) Characteristics and causes of crest cracking on a high core-wall rockfill dam: a case study. Eng Geol 297:106488

27. Cavuslu M (2022) Examination of 3D finite difference analyses of Zonguldak–Kozlu CCR dam subjected strong ground motions considering dam-foundation-reservoir interaction. Bitlis Eren Univ J Sci. 11(4):1117–1137

Publisher's Note Springer Nature remains neutral with regard to jurisdictional claims in published maps and institutional affiliations.